REVIEWS OF
MODERN PHYSICS

VOLUME 19, NUMBER 4 OCTOBER, 1947

Neutron Cross Sections of the Elements

A Compilation*

H. H. GOLDSMITH
Brookhaven National Laboratory, Upton, Long Island, New York

H. W. IBSER
University of Wisconsin, Madison, Wisconsin

AND

B. T. FELD
Physics Department and Laboratory for Nuclear Science and Engineering, Massachusetts Institute of Technology, Cambridge, Massachusetts

PRIOR to the war, most cross-section measurements at low neutron energies were made for distributions ranging around 1/40 ev (thermal neutrons).[1–4] There were, in addition, some measurements in the resonance region (1–1000 ev) made with various resonance detectors and boron-absorption techniques.[1,5–8] At high energies, measurements were made in essentially three energy regions: between 0.1 and 1 Mev, by use of photo-neutrons derived from naturally radioactive gamma-sources;[9,10] the region between 2 and 3 Mev, with neutrons derived from low voltage apparatus and the D(*d*,*n*) reaction;[11–13] finally, the very broad energy distribution, averaging around 4 Mev, obtained from Ra–Be sources.[3]

However, the nuclear physicist's interest in the study of nuclear energy levels, level spacing, level widths, etc., demands greater detail in the determination of cross section as a function of

* A collection of neutron cross sections of the elements, based on the prewar and wartime work of many investigators, was compiled during 1945 (by Goldsmith and Ibser) at the Metallurgical Laboratory, University of Chicago. This compilation was designed for use in the Manhattan Project Laboratories. It was declassified in June, 1946, for publication in the Manhattan Project Technical Series. Informal circulation resulted in widespread demand for the publication of such a collection. However, many of the original articles were then being prepared for appearance in the periodical literature. The publication of this collection was, therefore, delayed to permit as many as possible of these papers to appear in the normal fashion. During this delay the original collection was completely revised (by Feld and Goldsmith). At the present writing, some of the data included in this compilation are still unpublished, mainly because of the pressure of other commitments on the original authors. In all such cases, permission has been secured from the authors for the inclusion of their data in this collection.

[1] H. A. Bethe, Rev. Mod. Phys. 9, 69 (1937).
[2] K. Diebner, W. Herrmann, and E. Grassmann, Phys. Zeits. **43**, 440 (1942).
[3] J. R. Dunning, G. B. Pegram, G. A. Fink, and D. P. Mitchell, Phys. Rev. **48**, 265 (1935).
[4] H. Volz, Zeits. f. Physik **121**, 201 (1943).
[5] O. R. Frisch and G. Placzek, Nature **137**, 357 (1936).
[6] J. Hornbostel, H. H. Goldsmith, and J. H. Manley, Phys. Rev. **58**, 18 (1940).
[7] J. H. Manley, H. H. Goldsmith, and J. S. Schwinger, Phys. Rev. **55**, 39 (1939).
[8] R. Peierls, Reports on Progress in Physics **VII**, 87 (1940).
[9] W. E. Good and G. Scharff-Goldhaber, Phys. Rev. **59**, 917 (1941).
[10] A. I. Leipunsky, J. Phys. U.S.S.R. **3**, 231 (1940).
[11] H. Aoki, Proc. Phys. Math. Soc. Japan **21**, 232 (1939).
[12] M. R. MacPhail, Phys. Rev. **57**, 669 (1940).
[13] W. H. Zinn, S. Seely, and V. W. Cohen, Phys. Rev. **56**, 260 (1939).

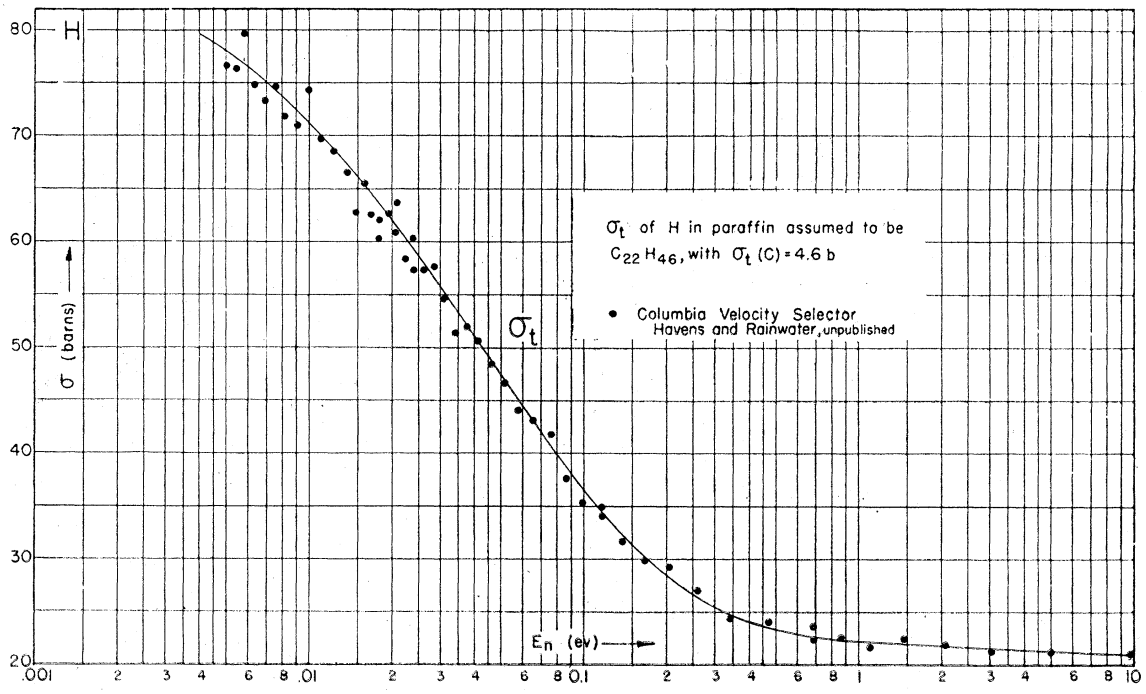
H
σ (barns)
σ_t
σ_t of H in paraffin assumed to be
$C_{22}H_{46}$, with σ_t (C) = 4.6 b
Columbia Velocity Selector
Havens and Rainwater, unpublished
E_n (ev)

FIG. 1.

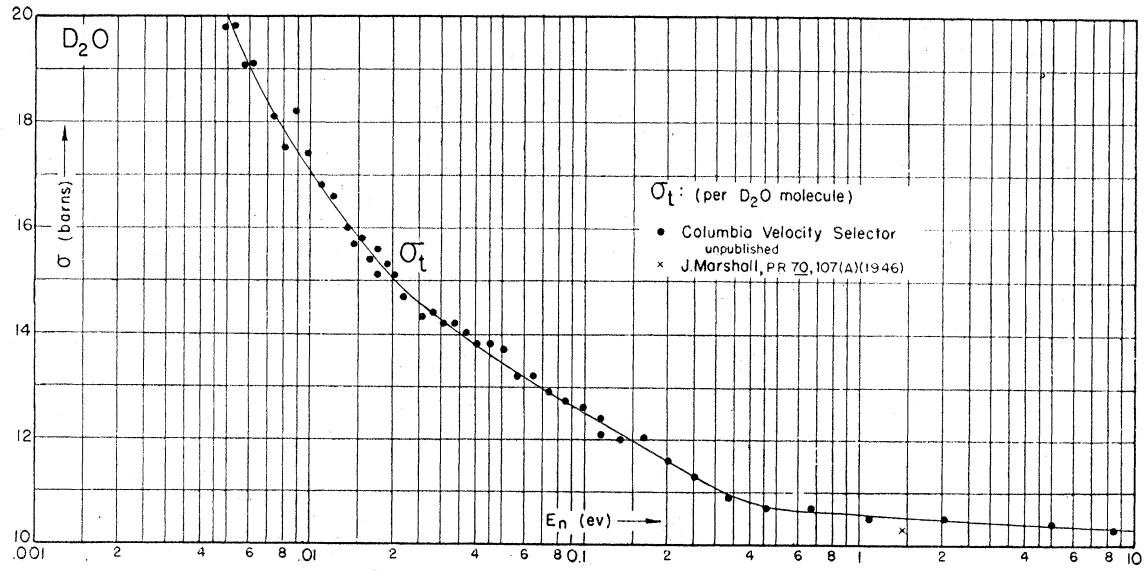
D_2O
σ (barns)
σ_t
σ_t: (per D_2O molecule)
Columbia Velocity Selector
unpublished
J. Marshall, PR 70, 107(A)(1946)
E_n (ev)

FIG. 3.

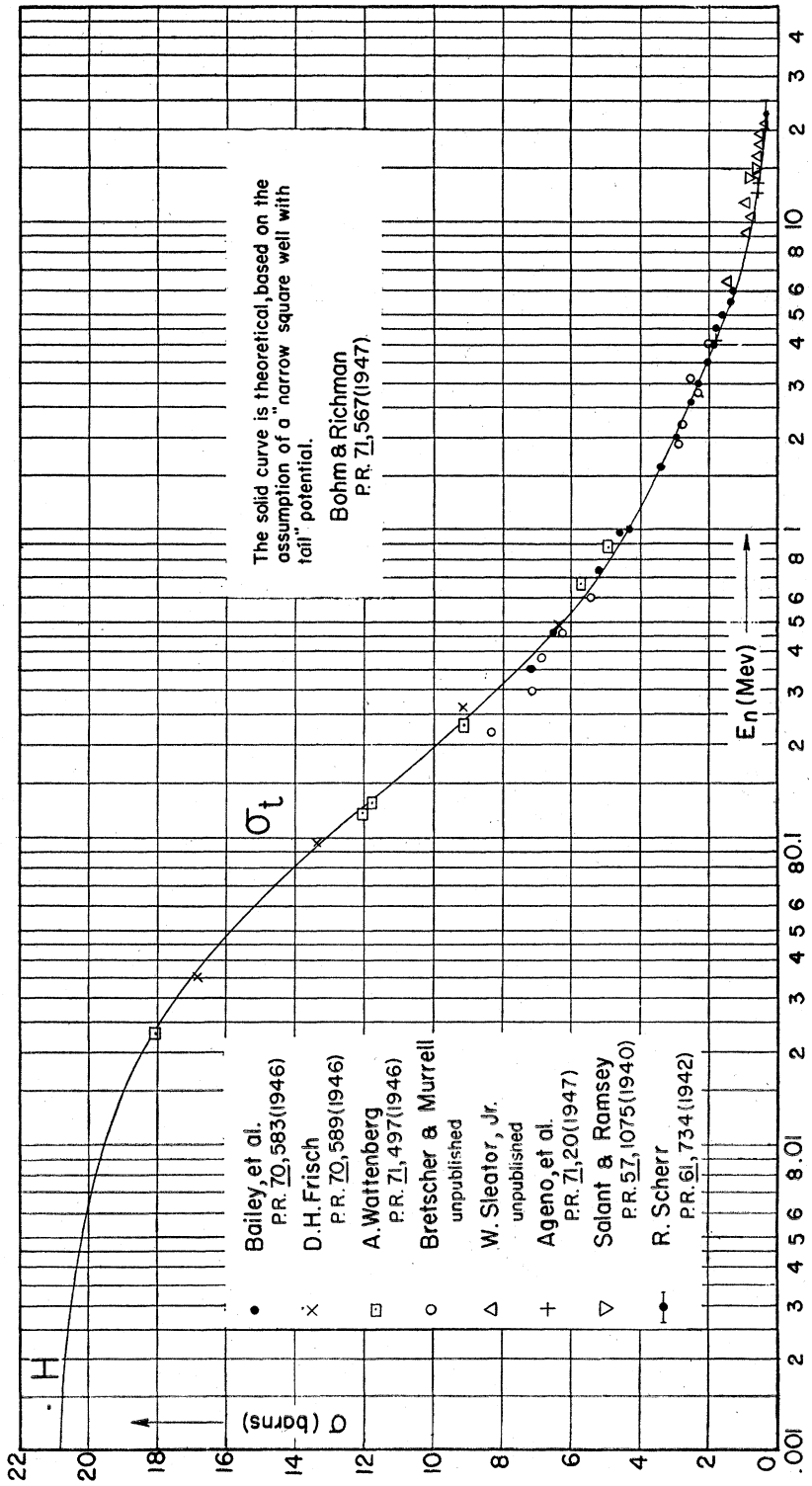

FIG. 2. (See "Note added in proof.")

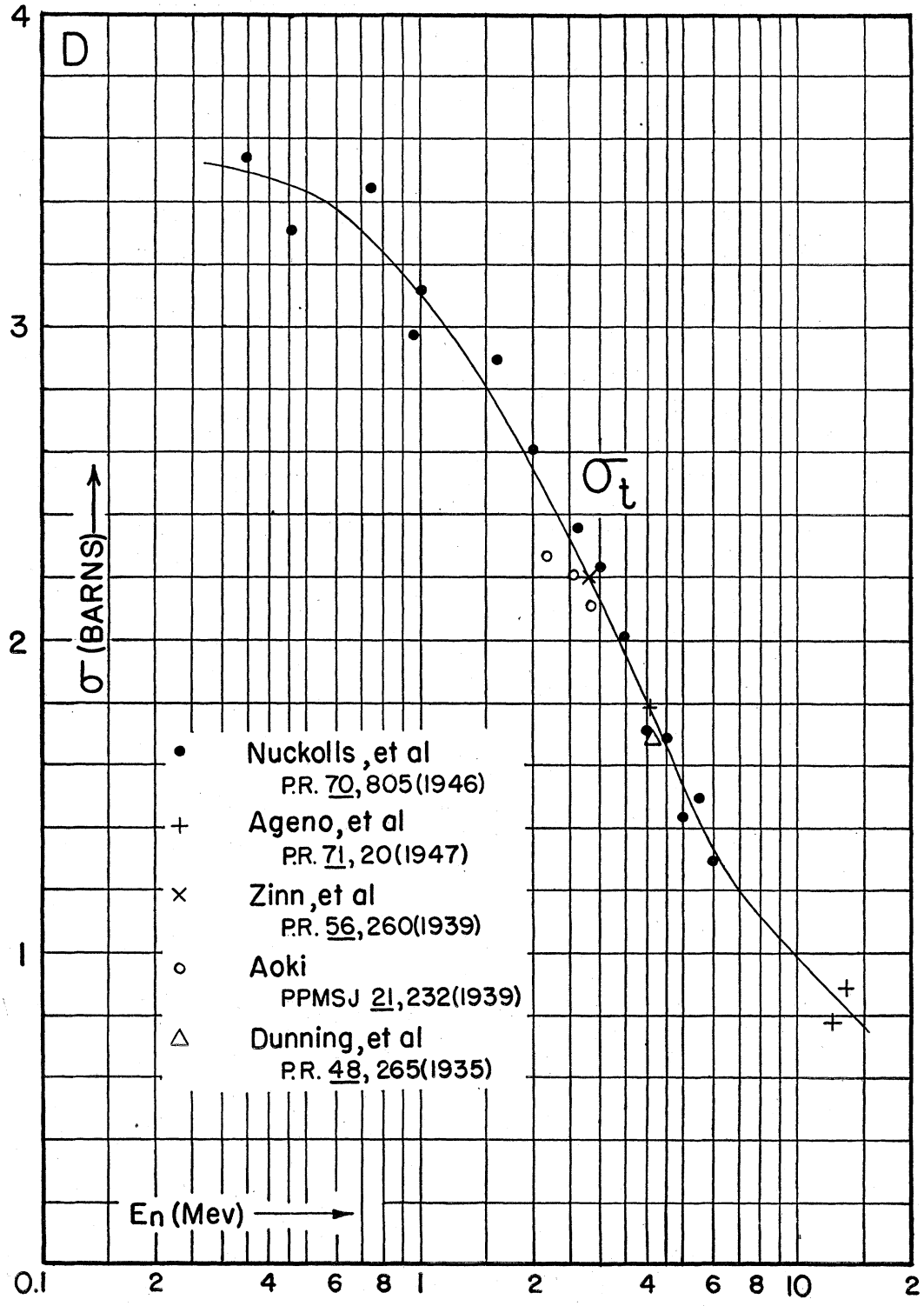
D
σ_t
σ (BARNS)
En (Mev)
Nuckolls, et al
P.R. 70, 805(1946)
Ageno, et al
P.R. 71, 20(1947)
Zinn, et al
P.R. 56, 260(1939)
Aoki
PPMSJ 21, 232(1939)
Dunning, et al
P.R. 48, 265(1935)
4
3
2
1
0.1
2
4
6
8
1
2
4
6
8
10
2

FIG. 4.

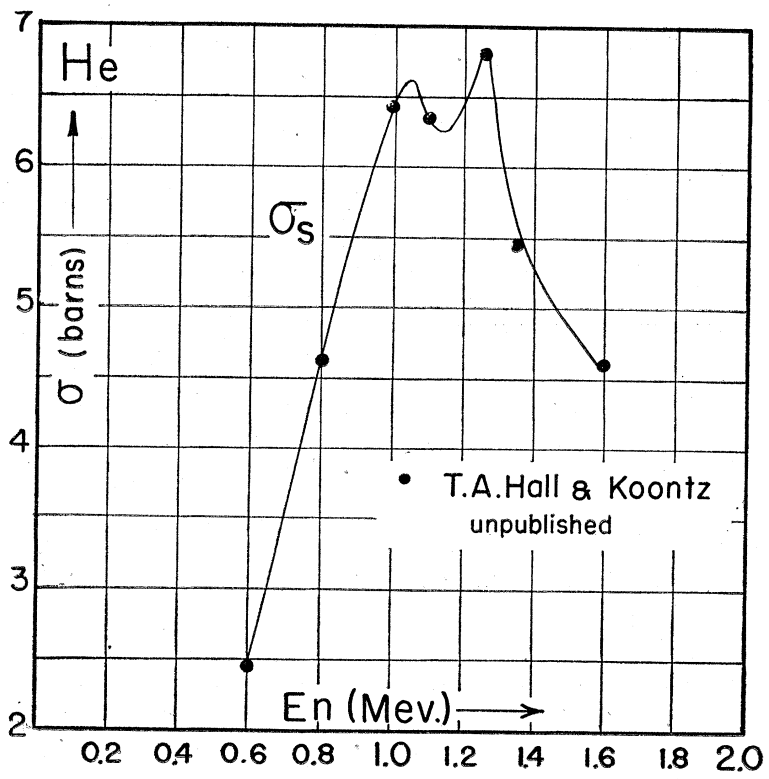

FIG. 5.
(See "Note added in proof.")

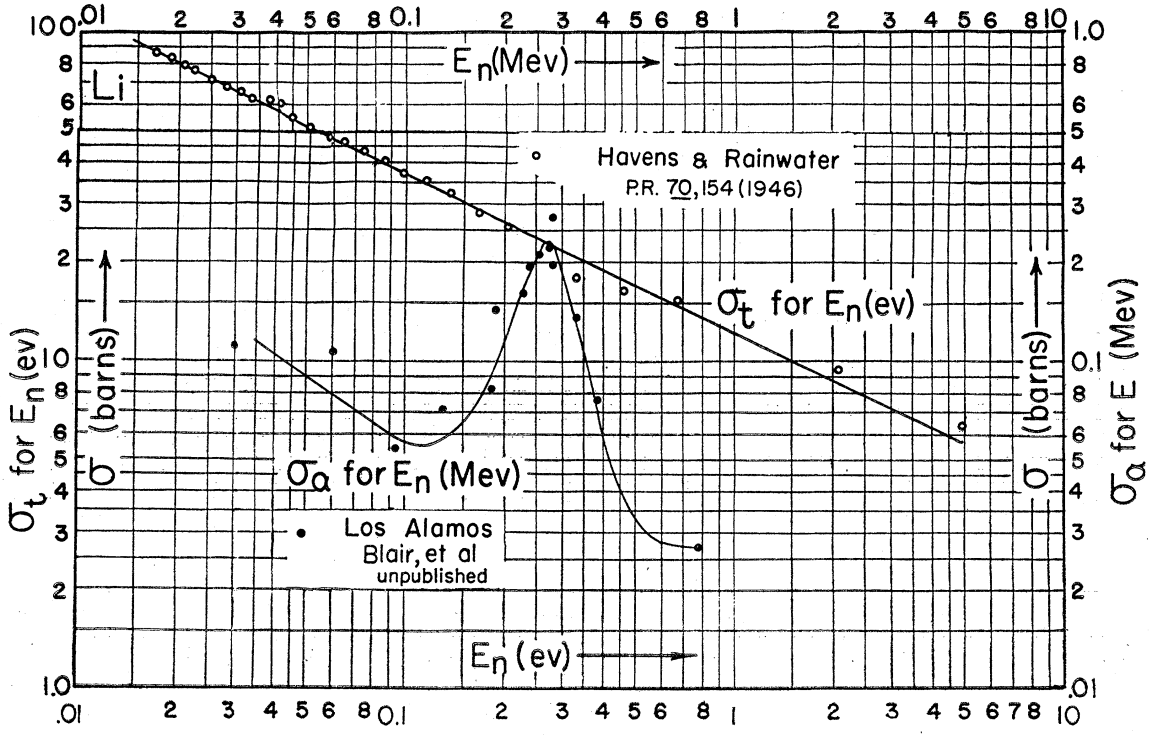

FIG. 6.

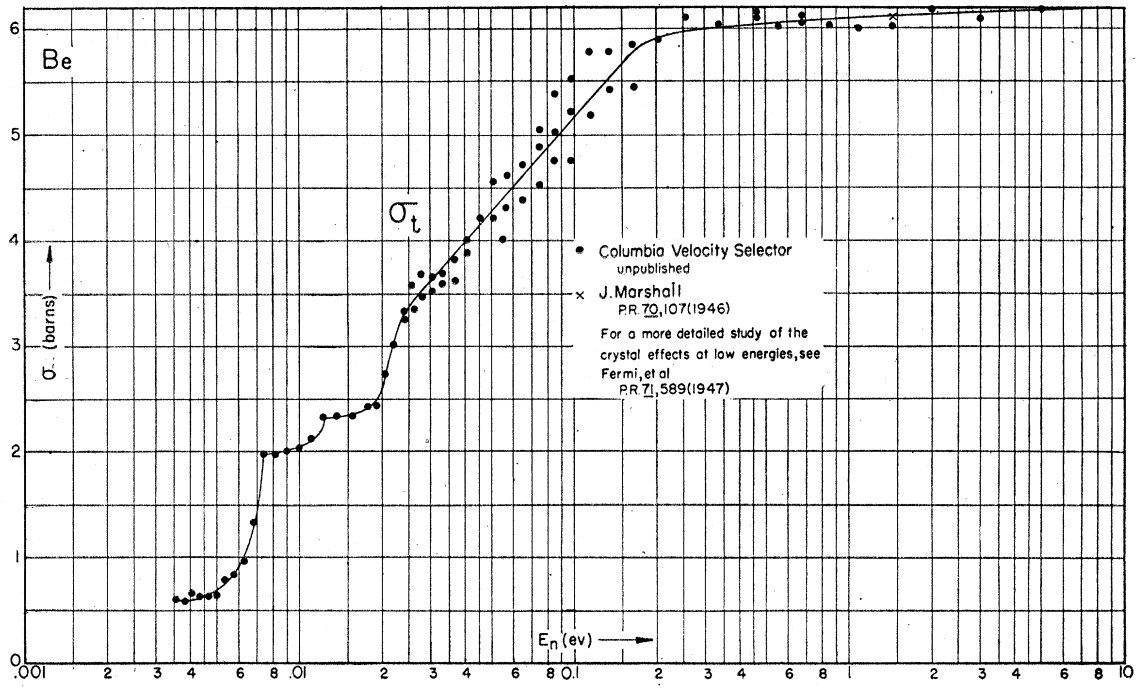
Be
σ_t
σ (barns)
Columbia Velocity Selector
unpublished
J. Marshall
P.R. 70, 107(1946)
For a more detailed study of the crystal effects at low energies, see
Fermi, et al
P.R. 71, 589(1947)
E_n (ev)

FIG. 7.

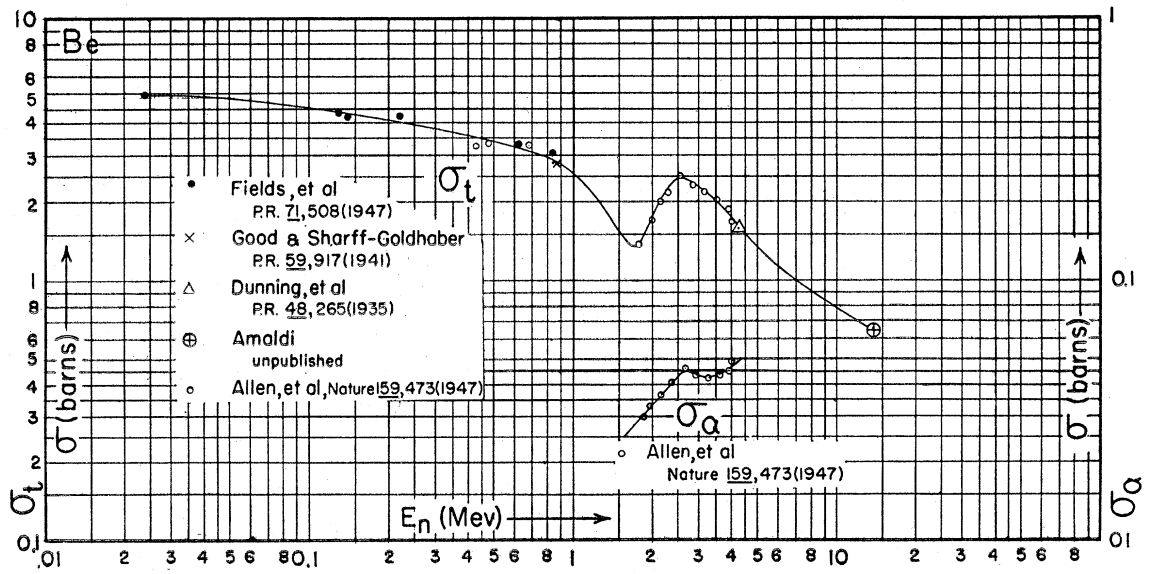
Be
Fields, et al
P.R. 71, 508(1947)
Good & Sharff-Goldhaber
P.R. 59, 917(1941)
Dunning, et al
P.R. 48, 265(1935)
Amaldi
unpublished
Allen, et al, Nature 159, 473(1947)
σ_t
σ_a
Allen, et al
Nature 159, 473(1947)
σ (barns)
E_n (Mev)

FIG. 8.

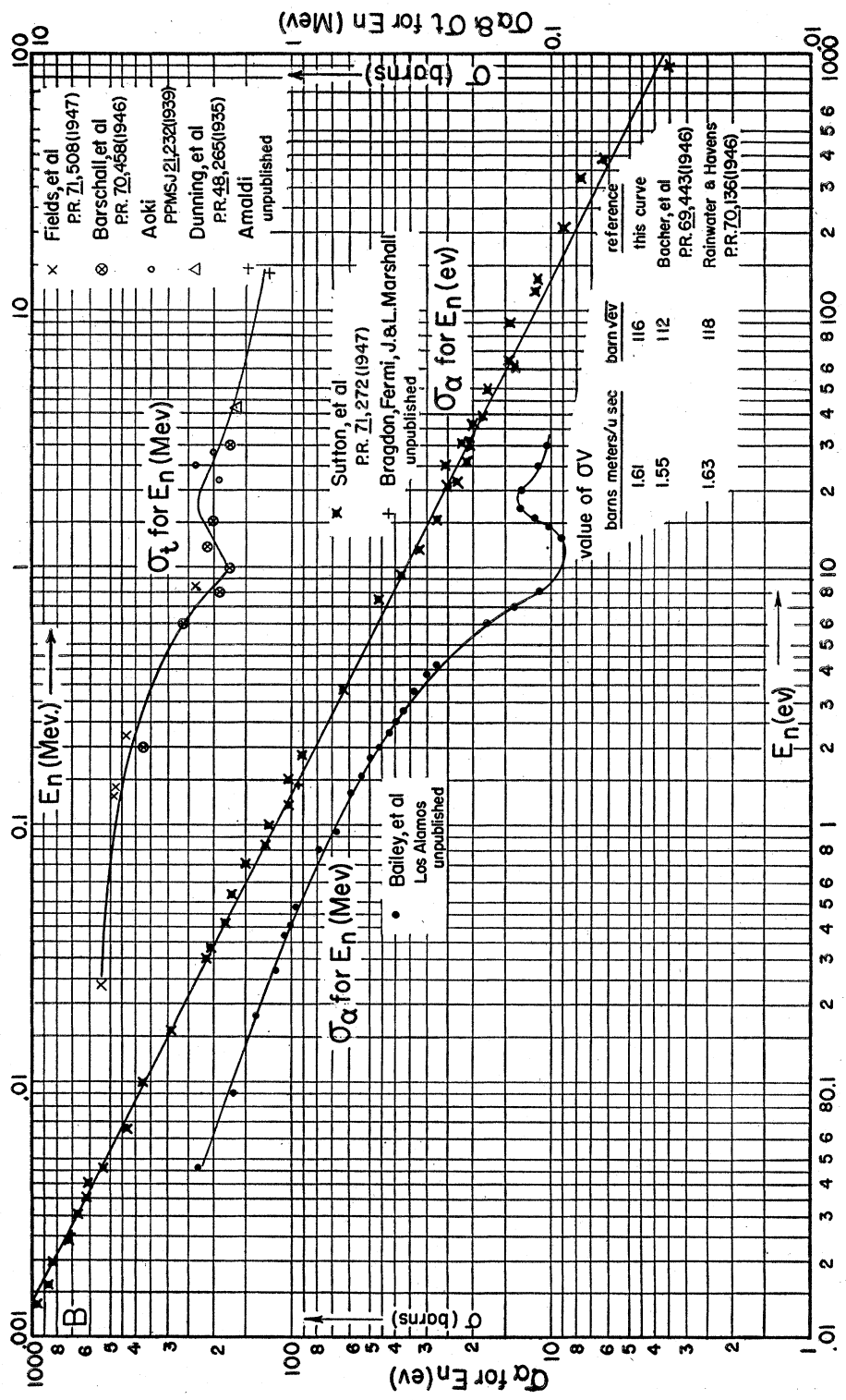

FIG. 9. (See "Note added in proof.")

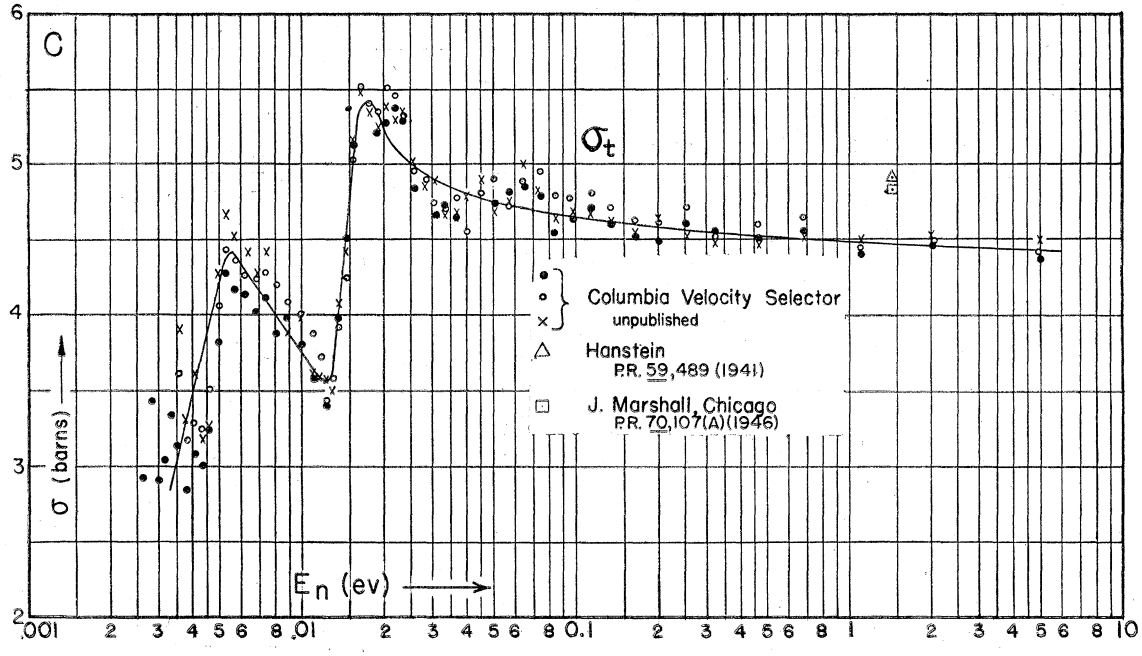

FIG. 10.

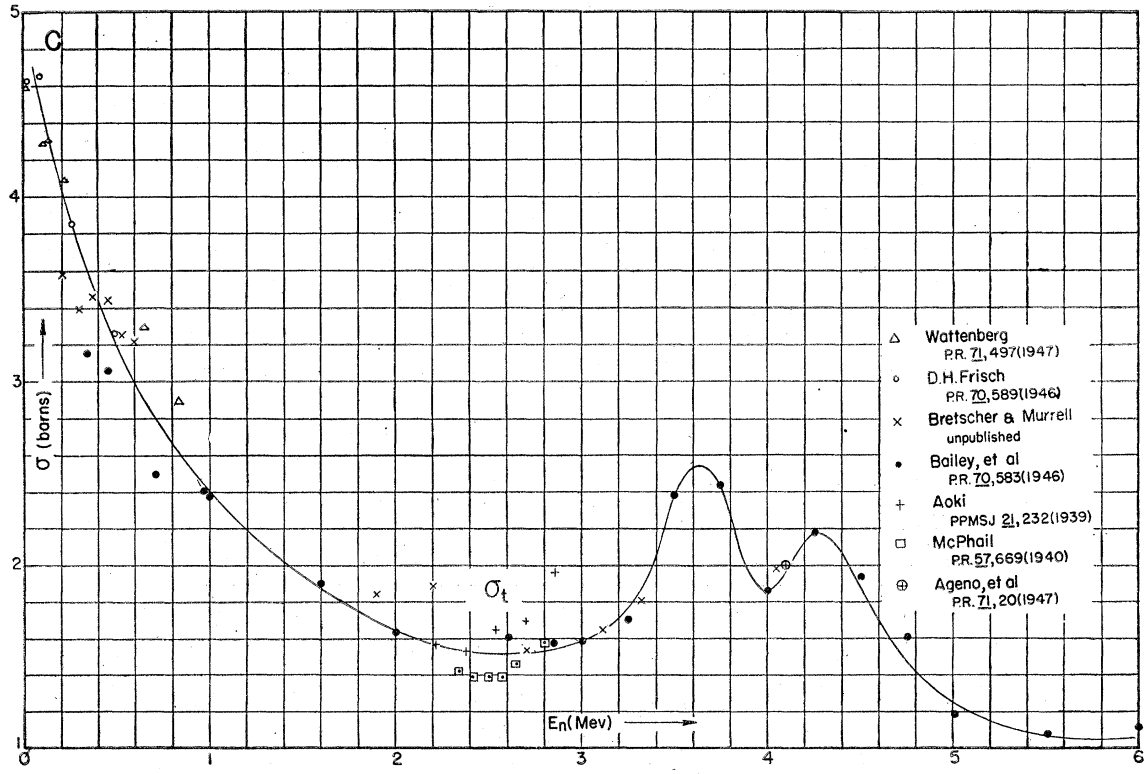

FIG. 11. (See "Note added in proof.")

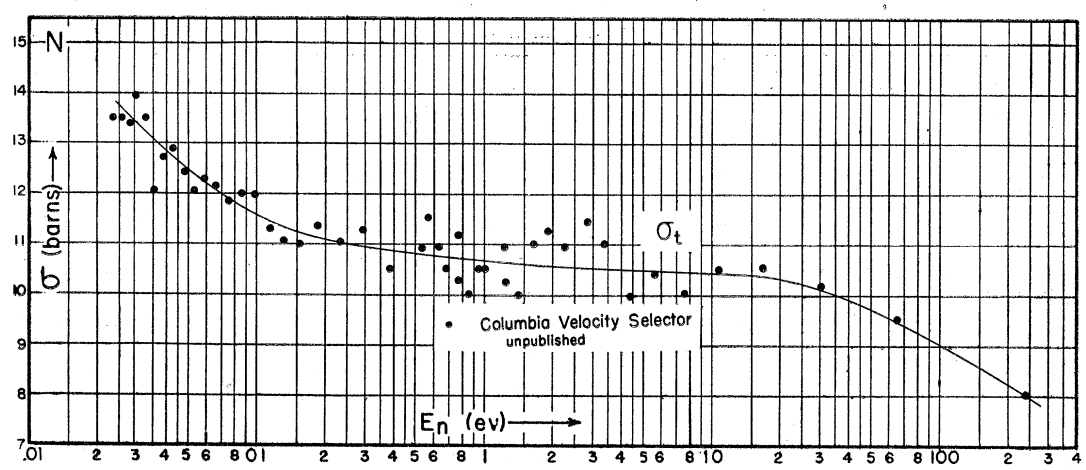
N
σ (barns)
σ_t
Columbia Velocity Selector
unpublished
E_n (ev)

FIG. 12.

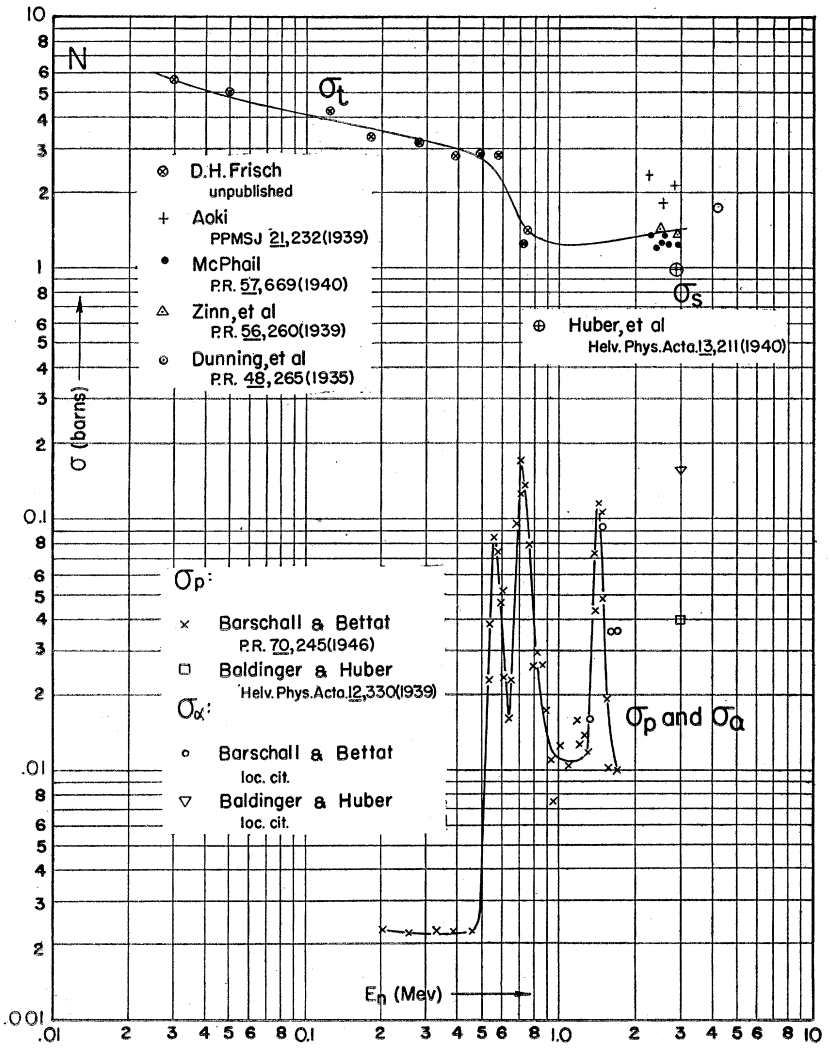
N
σ_t
D.H. Frisch
unpublished
Aoki
PPMSJ 21,232(1939)
McPhail
P.R. 57,669(1940)
Zinn, et al
P.R. 56,260(1939)
Dunning, et al
P.R. 48,265(1935)
Huber, et al
Helv. Phys. Acta. 13,211(1940)
σ_s
σ (barns)
σ_p:
Barschall & Bettat
P.R. 70,245(1946)
Baldinger & Huber
Helv. Phys. Acta. 12,330(1939)
σ_α:
Barschall & Bettat
loc. cit.
Baldinger & Huber
loc. cit.
σ_p and σ_α
E_n (Mev)

FIG. 13.

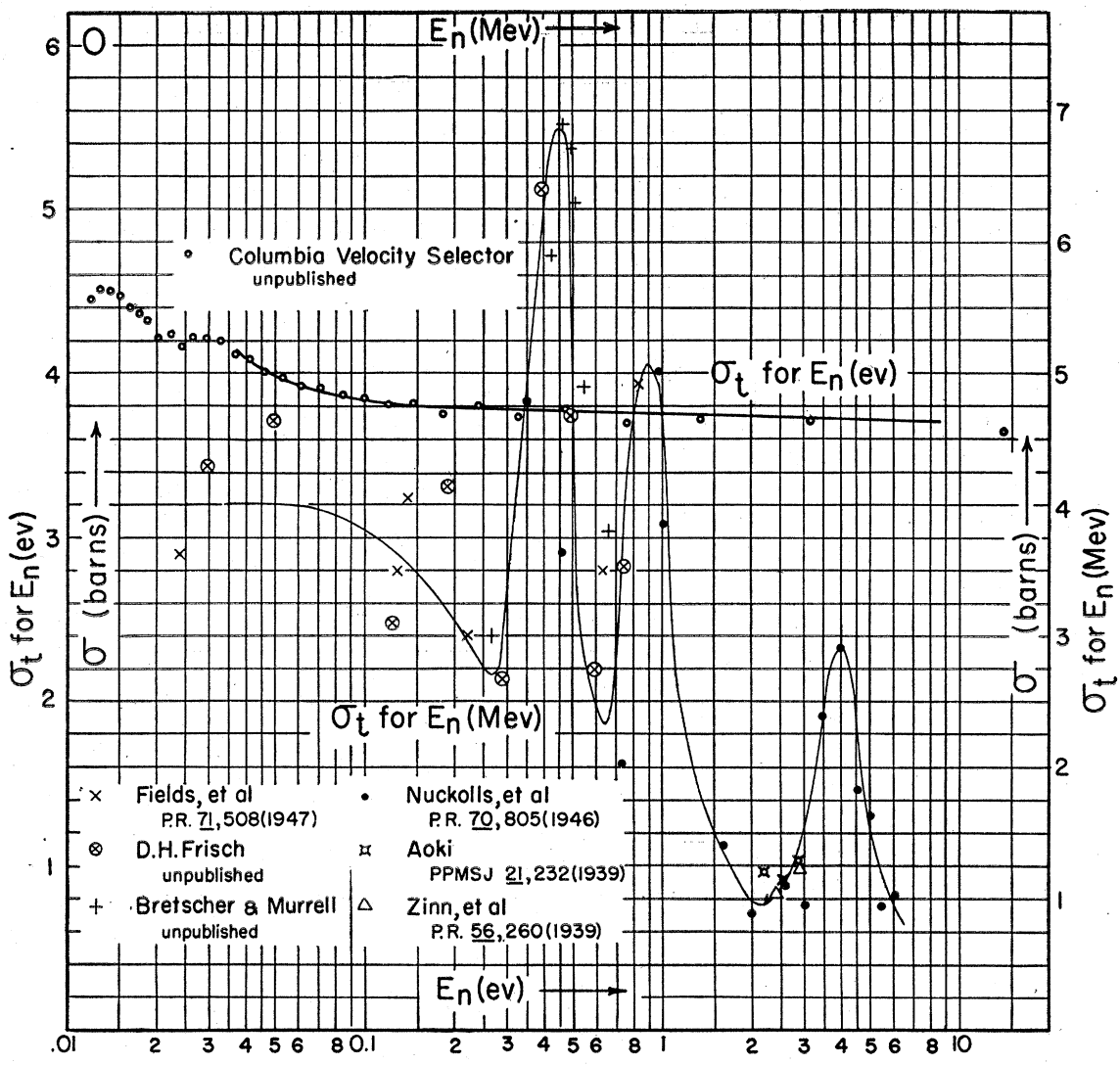

FIG. 14.

neutron energy. The technique of producing monoenergetic neutrons, already fairly well understood prior to the war,[14–19] was developed during the war in a number of directions, permitting the exploration of the low energy region (0–1000 ev), through the use of velocity selectors [time of flight, mechanical[20,21] and modulated-beam,[22–28] and crystal spectrometers[29,30]] and filtered neutron beams.[31] The high neutron intensities available from piles has been a useful

[14] L. W. Alvarez, Phys. Rev. **54**, 609 (1938).
[15] C. P. Baker and R. F. Bacher, Phys. Rev. **59**, 332 (1941).
[16] J. R. Dunning, G. B. Pegram, G. A. Fink, D. P. Mitchell, and E. Segrè, Phys. Rev. **48**, 704 (1935).
[17] G. E. F. Fertel, D. F. Gibbs, P. B. Moon, G. P. Thomson, and C. E. Wynn-Williams, Proc. Roy. Soc. **A175**, 316 (1940).
[18] L. J. Haworth, J. H. Manley, and E. A. Luebke, Rev. Sci. Inst. **12**, 591 (1941).
[19] J. M. W. Milatz and D. T. J. ter Horst, Physica **5**, 796 (1938).
[20] T. Brill and H. V. Lichtenberger, Phys. Rev. **72**, 585 (1947).
[21] E. Fermi, J. Marshall, and L. Marshall, Phys. Rev. **72**, 193 (1947).
[22] B. D. McDaniel, R. B. Sutton, L. S. Lavatelli, and E. E. Anderson, Phys. Rev. **72**, 729 (1947).
[23] W. W. Havens, Jr. and L. J. Rainwater, Phys. Rev. **70**, 154 (1946).
[24] W. W. Havens, Jr., C. S. Wu, L. J. Rainwater, and C. L. Meaker, Phys. Rev. **71**, 165 (1947).
[25] L. J. Rainwater and W. W. Havens, Jr., Phys. Rev. **70**, 136 (1946).

aid in the exploration of the low energy region. The investigation of the high energy region (30 kev to 6 Mev) was similarly aided through the emphasis on accurately controlled voltages in linear accelerators employing the Li(p,n) and D(d,n) reactions.[32–34] Furthermore, artificially produced isotopes emitting high energy γ-rays permitted the use of relatively monoenergetic neutrons in the 10-kev to 1-Mev region.[35]

Concurrent with these improvements in neutron sources and monochrometers, there have been advances in the techniques of neutron detection. The use of fission pulse ionization chambers, the availability of B^{10} for boron ionization chambers at low energies, the long counter for intermediate energies, and the use of either improved proportional counters depending on proton recoils or of threshold detectors at high neutron energies, have all contributed to the possibility of accurate cross-section measurements.

Although we have tried to include all of the pertinent data, some measurements may have been inadvertently excluded. In some cases, however, we have deliberately omitted a considerable body of data. (1) Since most of the prewar data in the low energy region have been superseded, we have not included these results. (2) There have more recently been more accurate measurements of activation cross sections, averaged over the thermal neutron (Maxwell) distribution. Most of these have employed, as thermal neutron sources, either piles[36] or Ra+Be neutrons slowed down in hydrogenous materials.[37] Since such measurements yield a single value representing the cross section averaged over a rather wide neutron energy range, and since thermal neutron cross sections may exhibit an erratic behavior in this region, because of resonances and crystal effects, the results obtained, though they are useful for many purposes, did not seem suitable for inclusion in this compilation. (3) Another example relates to the work of Leipunsky,[10] in which photo-neutrons were produced by the use of naturally radioactive sources. A comparison of these results with other work in the same region, and a consideration of the arguments used by Leipunsky to determine the neutron energies, indicate that the energies are not reliably estimated by him; nor is it possible for us to determine the effective neutron energies in his experiments. (4) Finally, the earlier measurements of Amaldi and co-workers, using the C(d,n) reaction,[38] were unreliable because their detectors were sensitive to gamma-rays as well as to neutrons.

Most of the curves included in this compilation are for the total cross section as a function of neutron energy; most of the measurements of cross section made with monoenergetic neutrons have been of the transmission type. In a number of instances, when specific reactions are easily detected (such as exothermic (n,p) or (n,α) reactions, fission, or reactions leading to detectable radioactive isotopes), the cross sections for these reactions have been determined as a function of the neutron energy.

The general plan of this survey has been to present the available cross-section data for each element in two curves, one containing the low energy (0.001–1000 ev) values, and the other the high energy (0.001–100 Mev). The cross sections plotted are in barns (10^{-24} cm^2) per atom of the normal element, except where otherwise indicated. In each case, the type of plot used has been chosen in order to allow the clearest representation of the data and to bring out the most important features of the energy variation of the cross section. The notation used has the following meaning: σ_t, total cross section, σ_s, scattering cross section, σ_τ, cross section for the

[26] L. J. Rainwater, W. W. Havens, Jr., C. S. Wu, and J. R. Dunning, Phys. Rev. **71**, 65 (1947).
[27] R. B. Sutton, B. D. McDaniel, E. E. Anderson, and L. S. Lavatelli, Phys. Rev. **71**, 272 (1947).
[28] C. S. Wu, L. J. Rainwater, and W. W. Havens, Jr., Phys. Rev. **71**, 174 (1947).
[29] L. B. Borst, A. J. Ulrich, C. L. Osborne, and B. Hasbrouck, Phys. Rev. **70**, 557 (1946).
[30] W. J. Sturm and G. P. Arnold, Phys. Rev. **71**, 556 (1947).
[31] H. L. Anderson, E. Fermi, and L. W. Marshall, Phys. Rev. **70**, 815 (1946).
[32] C. L. Bailey, W. E. Bennett, T. Bergstralh, R. G. Nuckolls, H. T. Richards, and J. H. Williams, Phys. Rev. **70**, 583 (1946).
[33] D. H. Frisch, Phys. Rev. **70**, 589 (1946).
[34] R. G. Nuckolls, C. L. Bailey, W. E. Bennett, T. Bergstralh, H. T. Richards, and J. H. Williams, Phys. Rev. **70**, 805 (1946).
[35] A. Wattenberg, Phys. Rev. **71**, 497 (1946).
[36] L. Seren, H. N. Friedlander, and S. H. Turkel, Phys. Rev. **72**, 888 (1947).
[37] J. W. Coltman and M. Goldhaber, Phys. Rev. **69**, 411 (1946).
[38] E. Amaldi, D. Bocciarelli, F. Rasetti, and G. C. Trabacchi, Phys. Rev. **56**, 881 (1939).

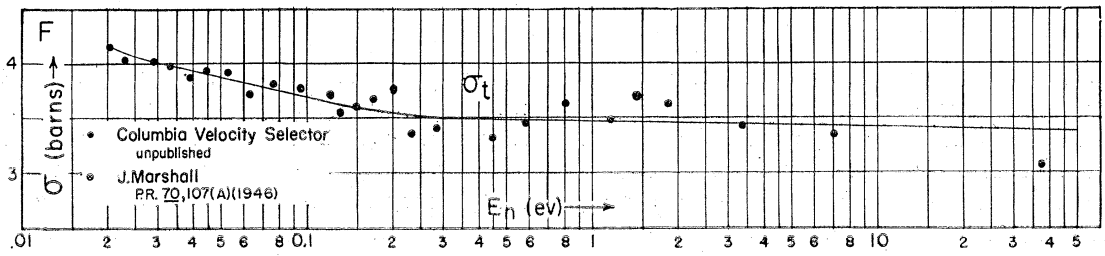
F
σ (barns)
σ_t
Columbia Velocity Selector
unpublished
J.Marshall
P.R. 70,107(A)(1946)
E_n (ev)

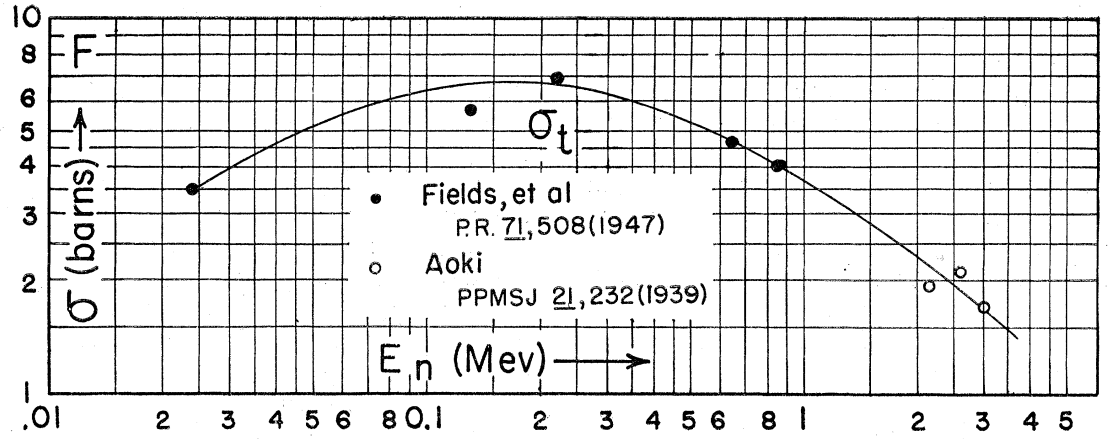
F
σ (barns)
σ_t
Fields, et al
P.R. 71,508(1947)
Aoki
PPMSJ 21,232(1939)
E_n (Mev)

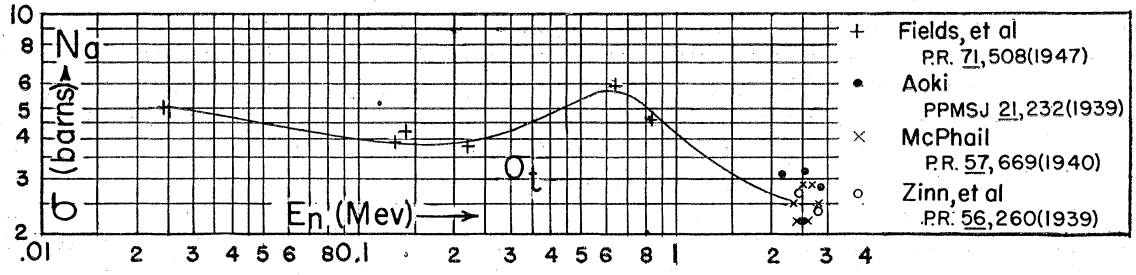
Na
σ (barns)
σ_t
E_n (Mev)
Fields, et al
P.R. 71,508(1947)
Aoki
PPMSJ 21,232(1939)
McPhail
P.R. 57,669(1940)
Zinn, et al
P.R. 56,260(1939)

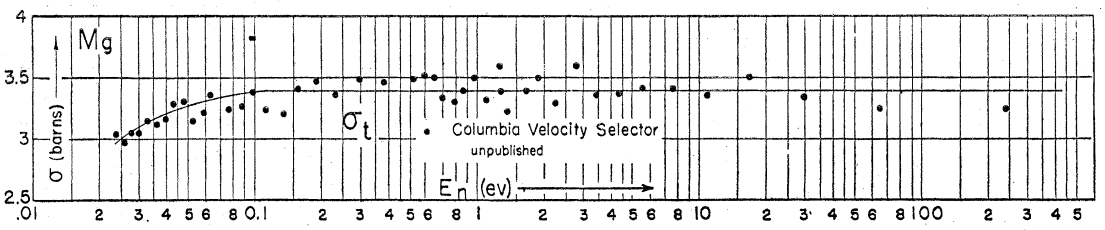
Mg
σ (barns)
σ_t
Columbia Velocity Selector
unpublished
E_n (ev)

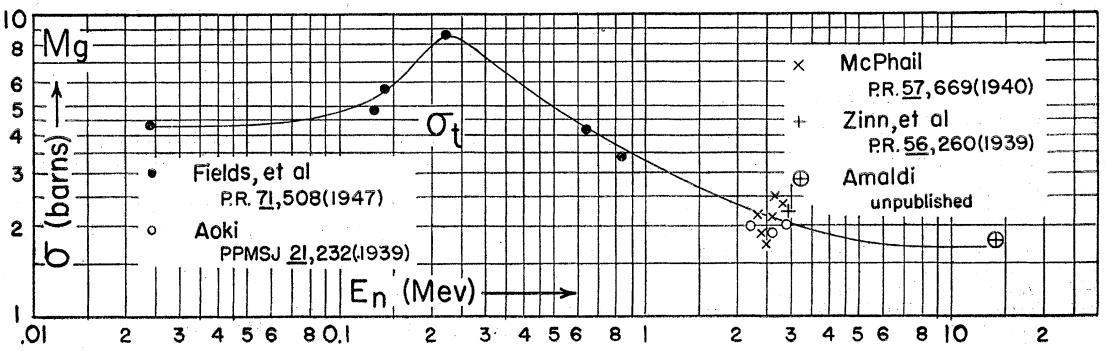
Mg
σ (barns)
σ_t
Fields, et al
P.R. 71,508(1947)
Aoki
PPMSJ 21,232(1939)
E_n (Mev)
McPhail
P.R. 57,669(1940)
Zinn, et al
P.R. 56,260(1939)
Amaldi
unpublished

FIGS. 15–19.

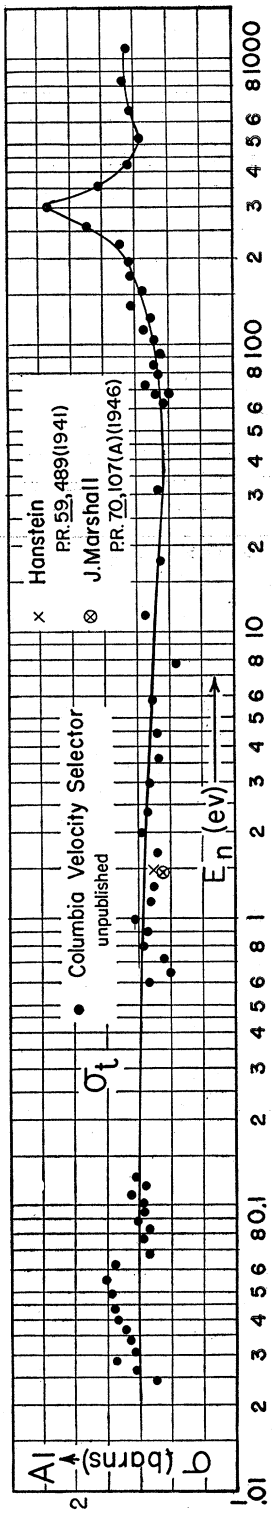

FIG. 20.

FIG. 21. (See "Note added in proof.")

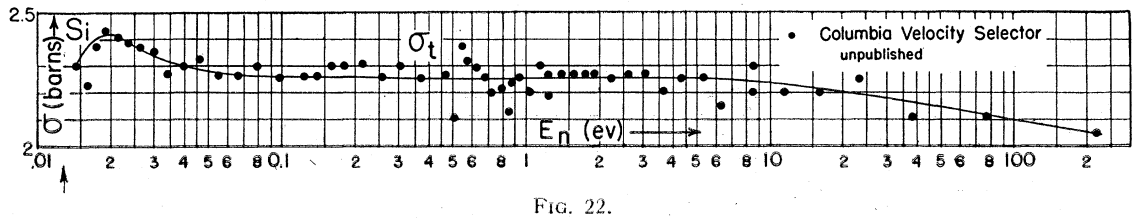

FIG. 22.

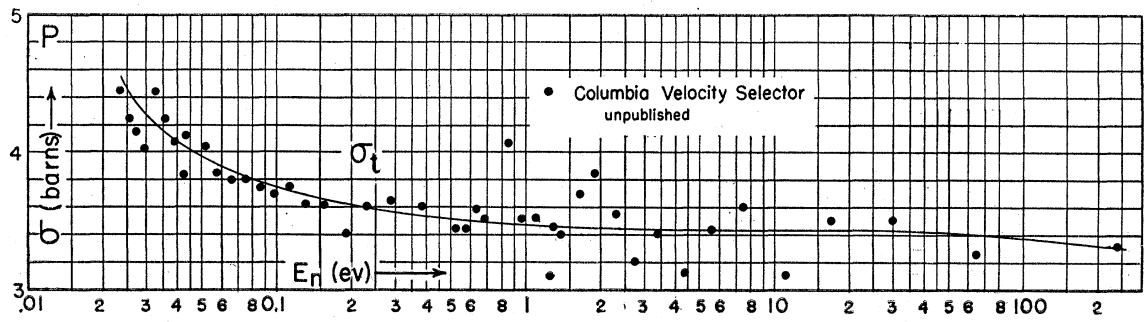

FIG. 23.

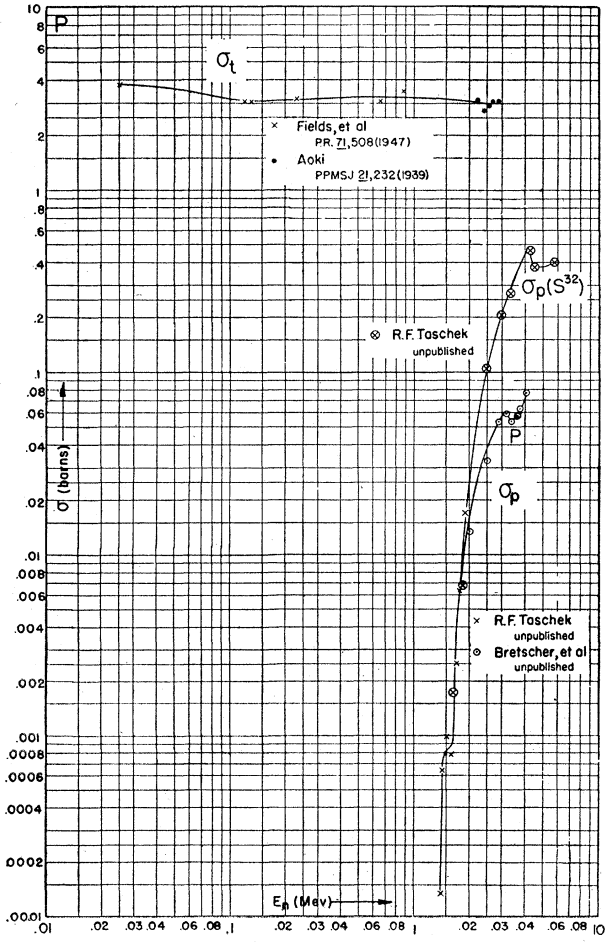

FIG. 24. (See "Note added in proof.")

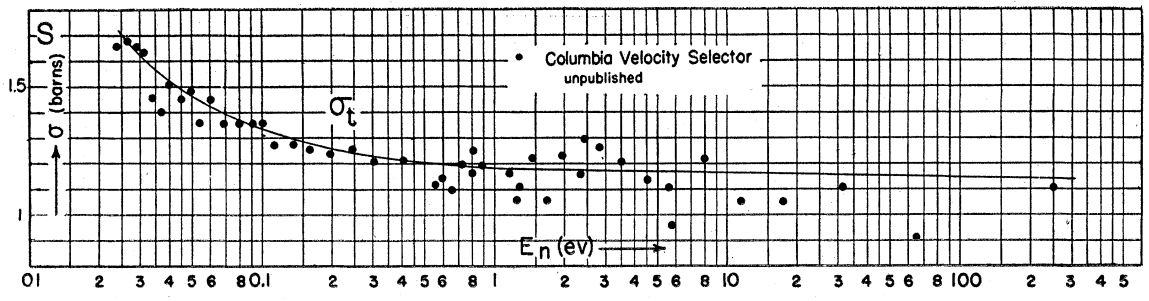

FIG. 25.

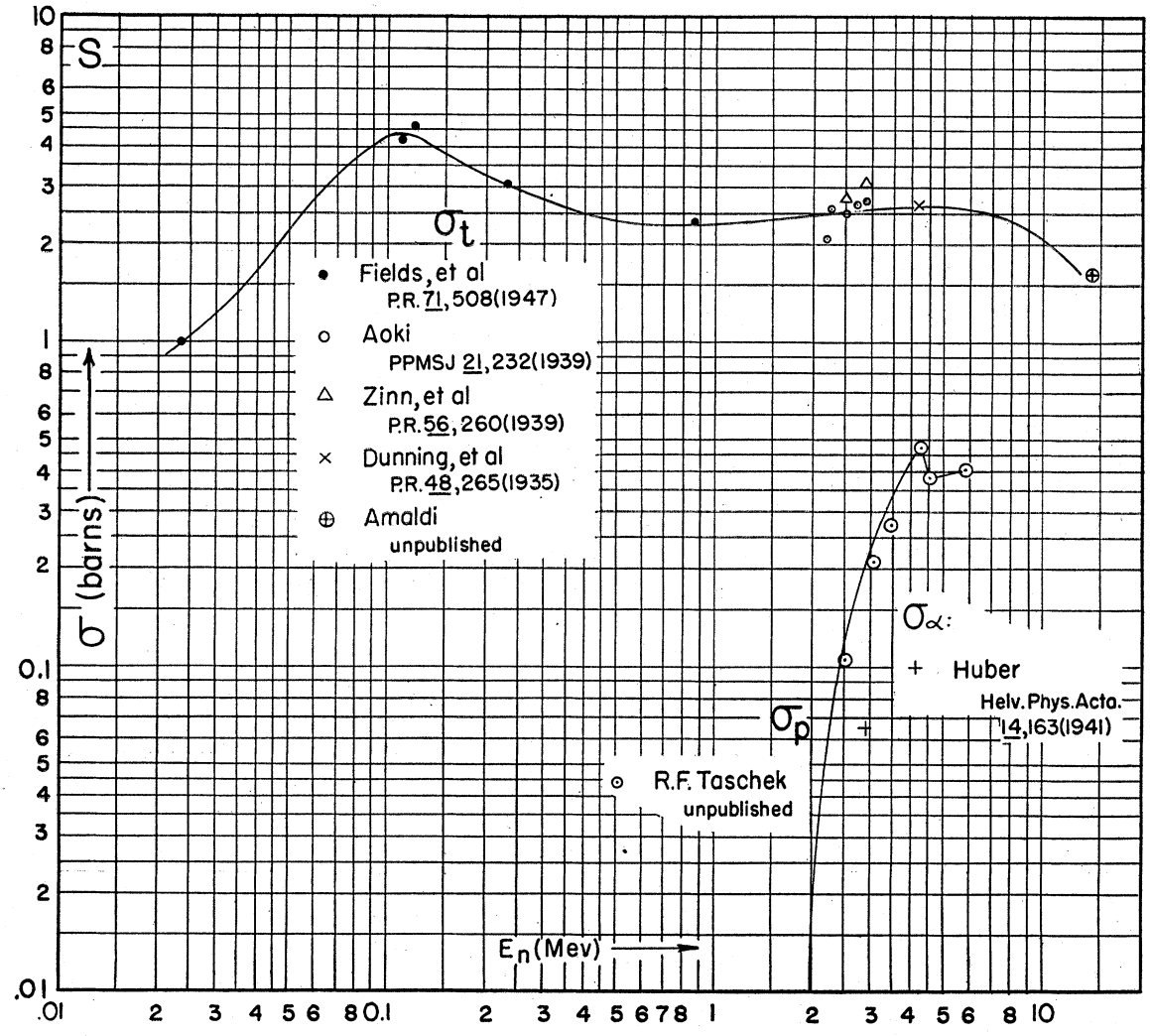

FIG. 26. (See "Note added in proof.")

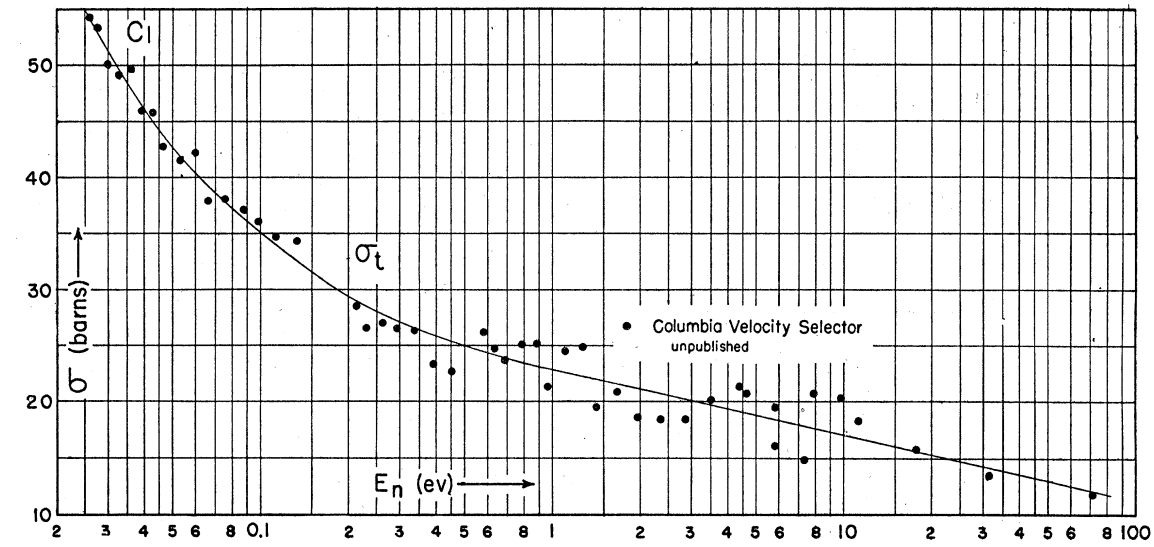
Cl
σt
σ (barns)
En (ev)
Columbia Velocity Selector
unpublished

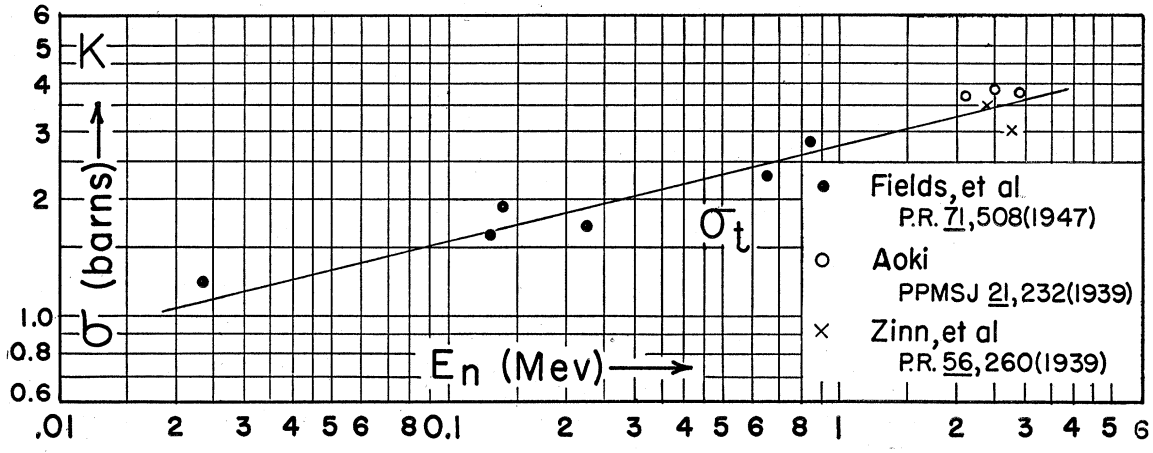
K
σ (barns)
σt
En (Mev)
Fields, et al
P.R. 71,508(1947)
Aoki
PPMSJ 21,232(1939)
Zinn, et al
P.R. 56,260(1939)

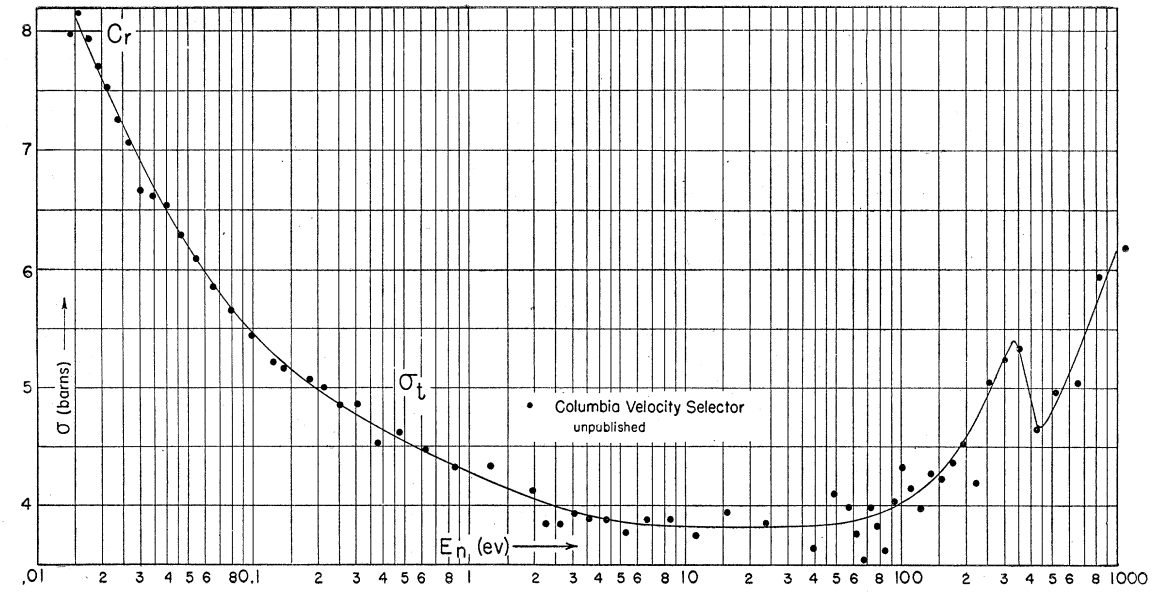
Cr
σt
σ (barns)
En (ev)
Columbia Velocity Selector
unpublished

FIGS. 27–29.

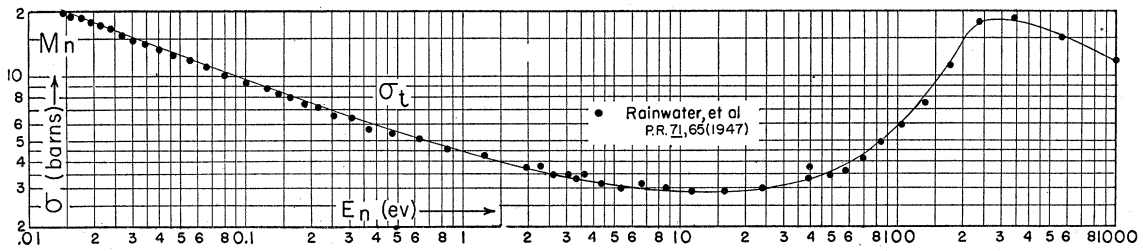
Mn
σt
σ (barns)
En (ev)
Rainwater, et al
P.R. 71, 65(1947)

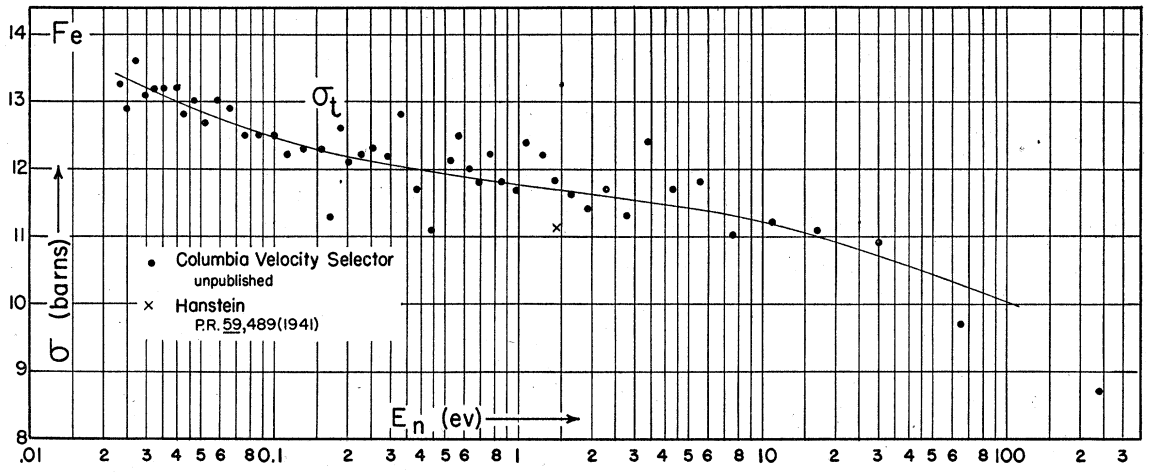
Fe
σt
σ (barns)
En (ev)
Columbia Velocity Selector
unpublished
Hanstein
P.R. 59, 489(1941)

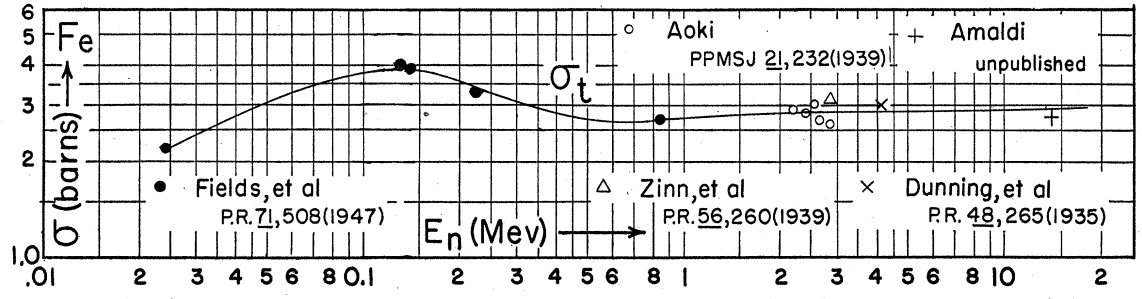
Fe
σt
σ (barns)
En (Mev)
Aoki
PPMSJ 21, 232(1939)
Amaldi
unpublished
Fields, et al
P.R. 71, 508(1947)
Zinn, et al
P.R. 56, 260(1939)
Dunning, et al
P.R. 48, 265(1935)

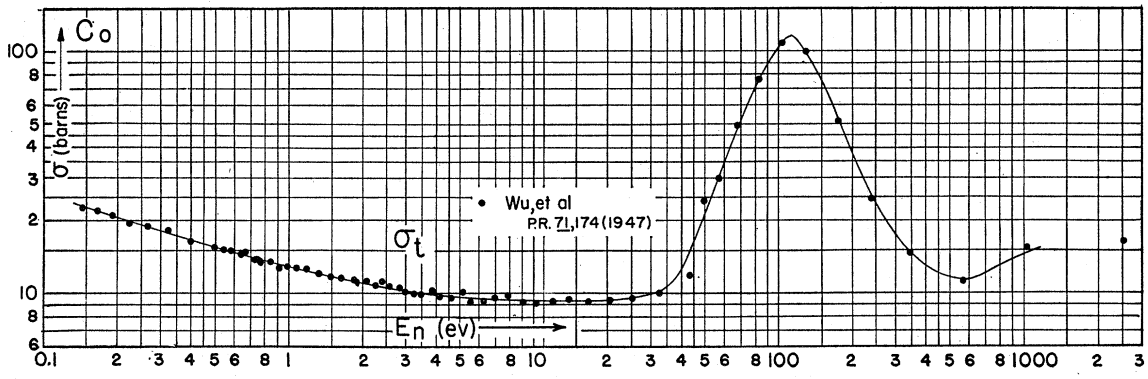
Co
σt
σ (barns)
En (ev)
Wu, et al
P.R. 71, 174(1947)

FIGS. 30–33.

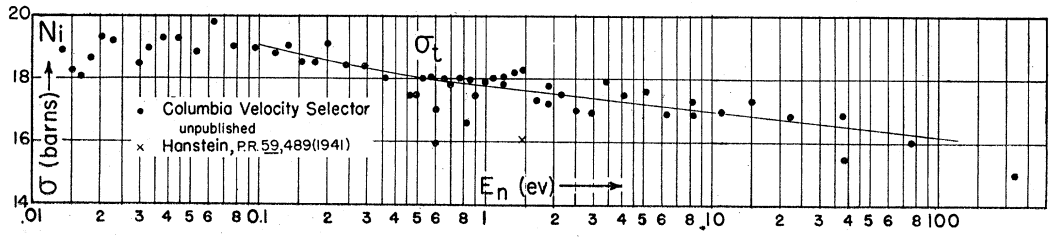
Ni
σ (barns)
σt
Columbia Velocity Selector
unpublished
Hanstein, P.R. 59, 489(1941)
En (ev)

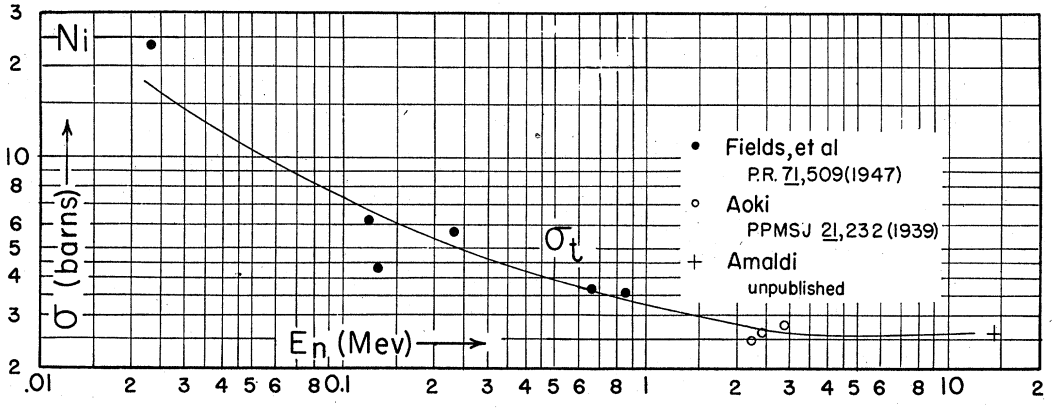
Ni
σ (barns)
σt
Fields, et al
P.R. 71, 509(1947)
Aoki
PPMSJ 21, 232(1939)
Amaldi
unpublished
En (Mev)

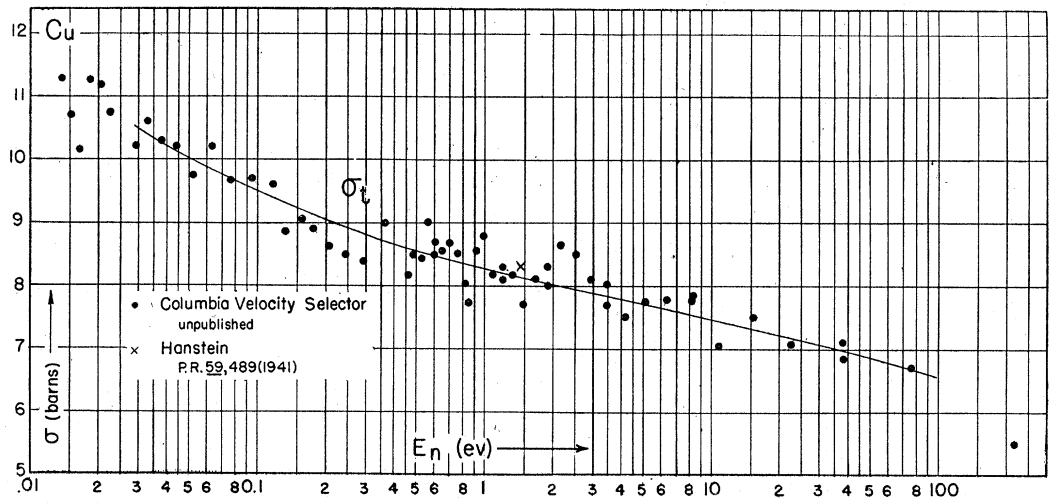
Cu
σ (barns)
σt
Columbia Velocity Selector
unpublished
Hanstein
P.R. 59, 489(1941)
En (ev)

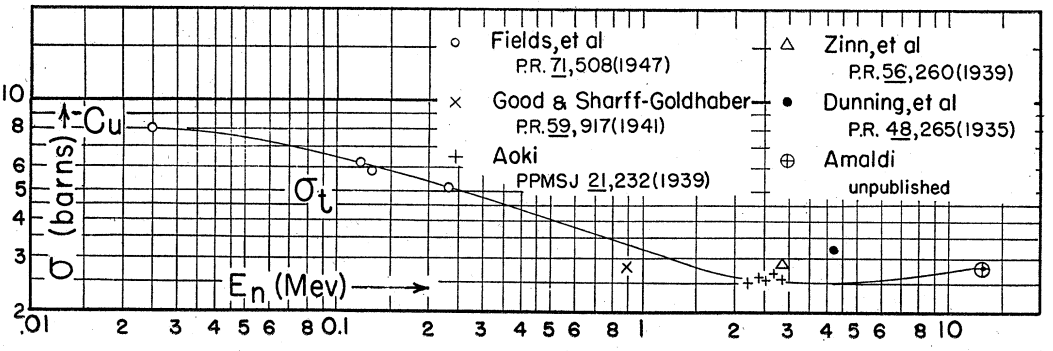
Cu
σ (barns)
σt
Fields, et al
P.R. 71, 508(1947)
Good & Sharff-Goldhaber
P.R. 59, 917(1941)
Aoki
PPMSJ 21, 232(1939)
Zinn, et al
P.R. 56, 260(1939)
Dunning, et al
P.R. 48, 265(1935)
Amaldi
unpublished
En (Mev)

FIGS. 34–37.

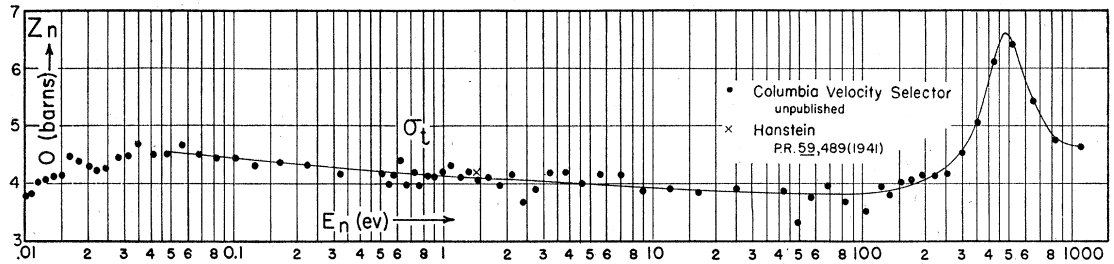
Zn
σ (barns)
σt
En (ev)
Columbia Velocity Selector
unpublished
Hanstein
P.R. 59,489(1941)

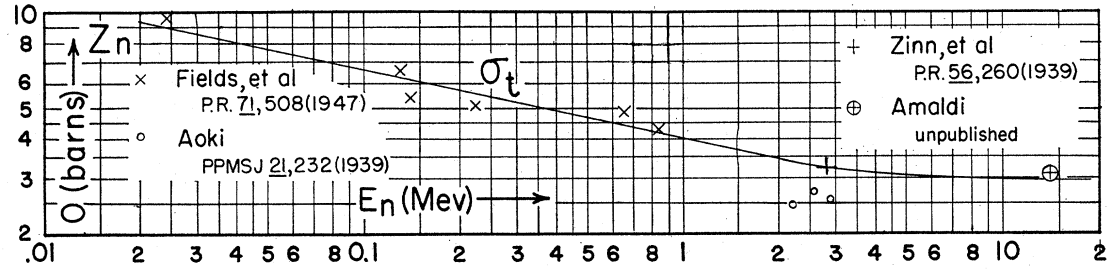
Zn
σ (barns)
σt
En (Mev)
Fields, et al
P.R. 71,508(1947)
Aoki
PPMSJ 21,232(1939)
Zinn, et al
P.R. 56,260(1939)
Amaldi
unpublished

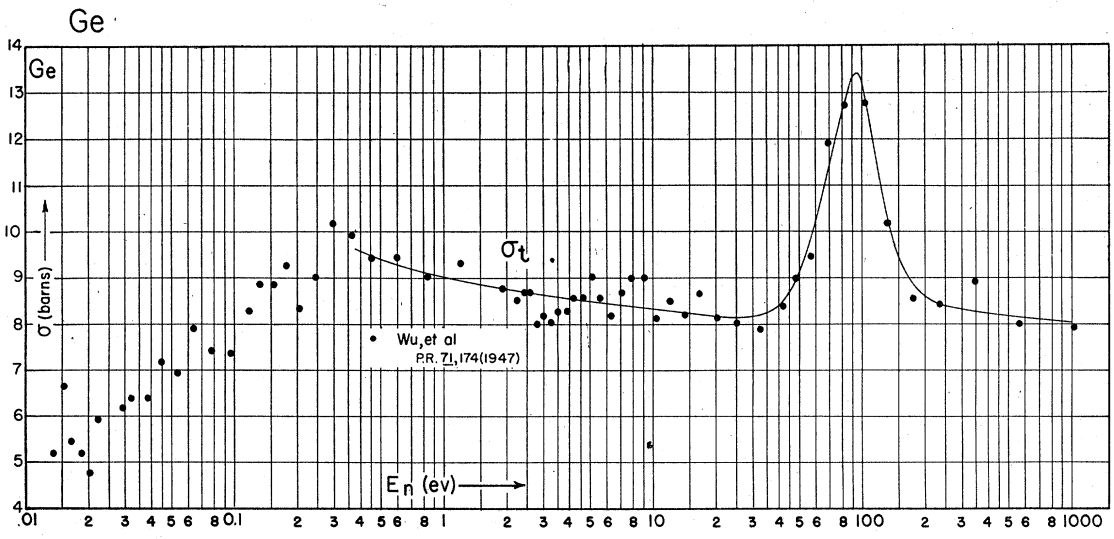
Ge
Ge
σ (barns)
σt
En (ev)
Wu, et al
P.R. 71,174(1947)

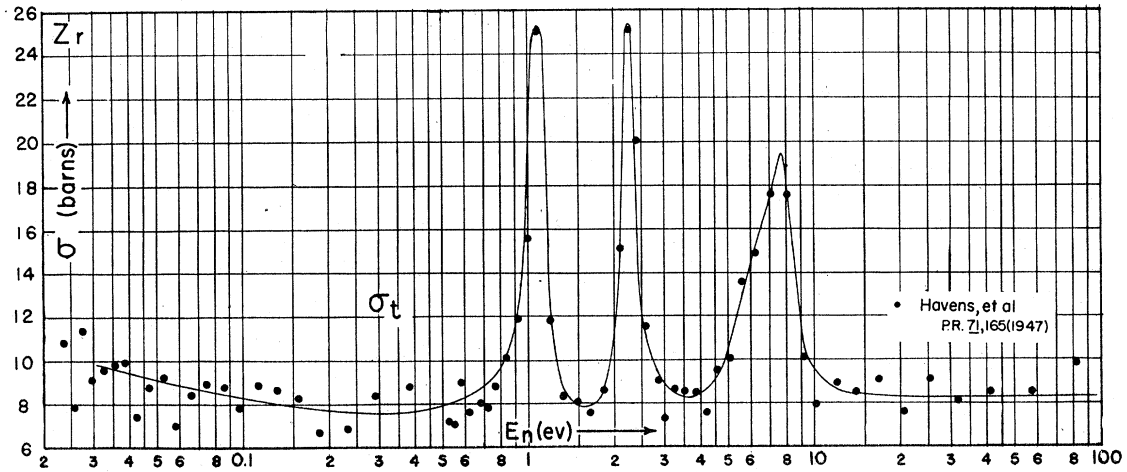
Zr
σ (barns)
σt
En (ev)
Havens, et al
P.R. 71,165(1947)

FIGS. 38–41.

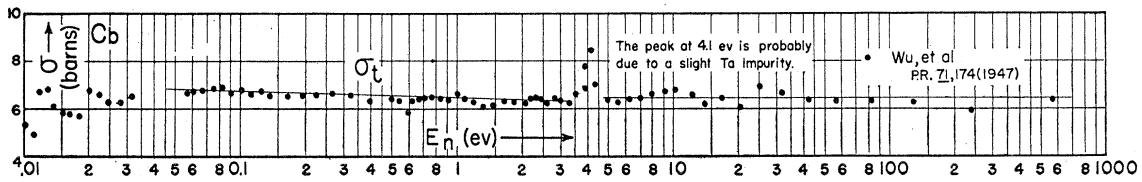

FIG. 42.

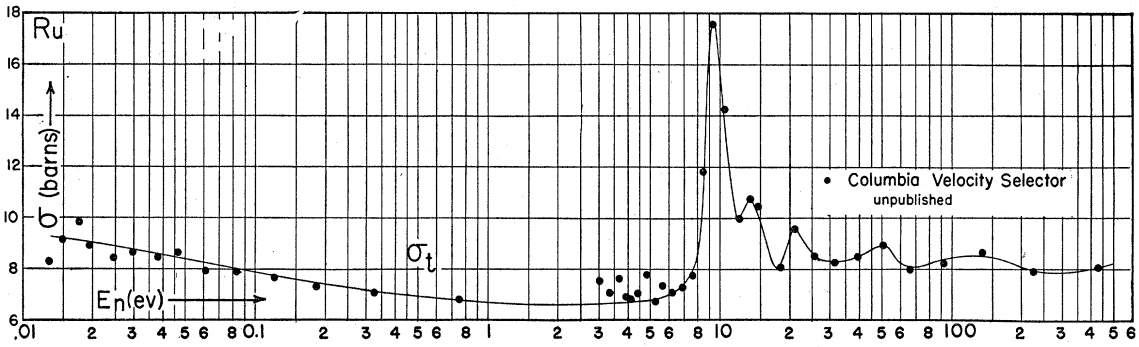

FIG. 43.

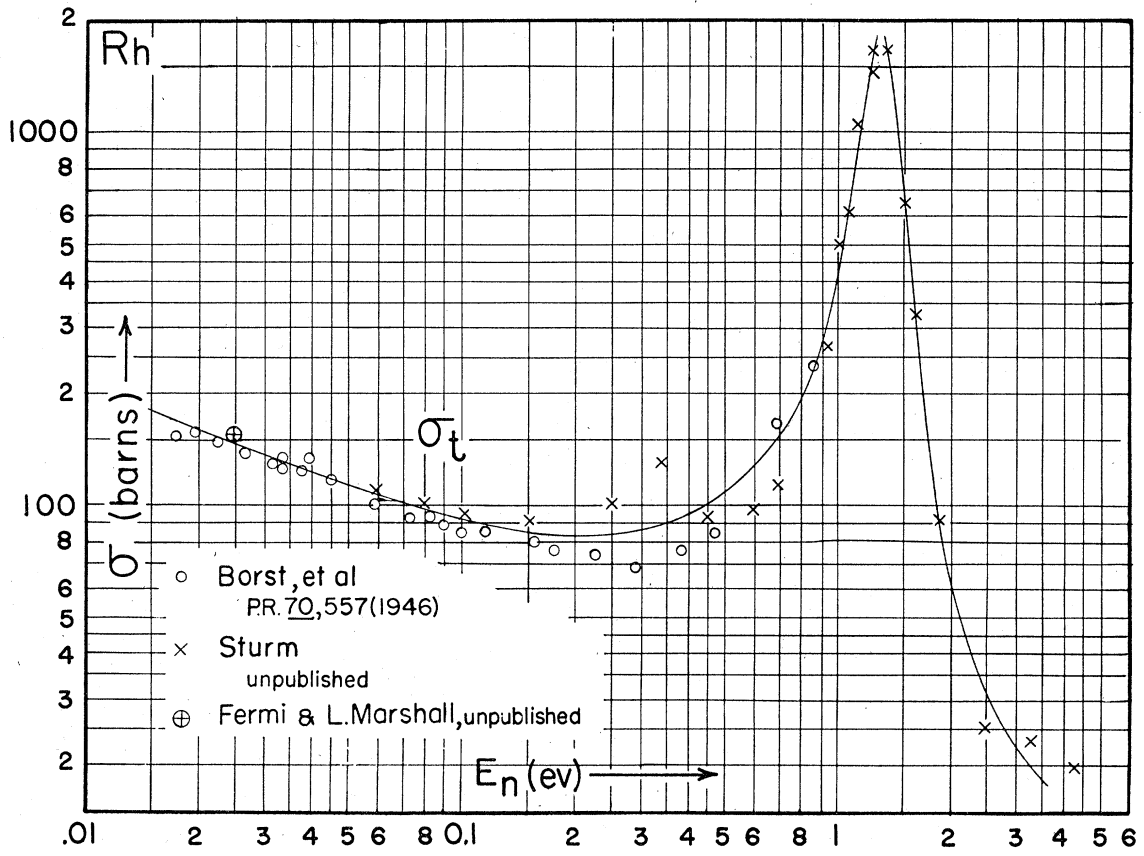

FIG. 44. (See "Note added in proof.")

(n,γ) process, σ_p, cross section for the (n,p) process, σ_α, cross section for the (n,α) process, σ_f, cross section for fission.

The curves of total cross section *versus* neutron energy in the low energy region fall into a small number of patterns. These can be understood in terms of relatively simple quantum-mechanical concepts, plus the statistical ideas of the compound nucleus, originally advanced by Bohr and expanded by the work of Breit and Wigner and others.[1,8,39–45] According to these ideas the total nuclear cross section for neutrons consists of a constant scattering cross section (potential scattering) superimposed on a variable cross section involving the formation of a compound nucleus. The formation of a compound nucleus by the addition of a neutron may result in a number of alternative reactions; the competition between these reactions is usually described in terms of the "reaction width." This is a measure of the probability (the inverse of the lifetime) for a given mode of disintegration of the compound nucleus, and may be understood in terms of the uncertainty principle $\Delta E\Delta t\cong\hbar$. Thus, the reaction width for an (n,x) process is defined as $\Gamma_x=\hbar/\tau_x$, where τ_x is the mean life of the compound nucleus against emission of the particle (or quantum) x; Γ_x has the dimensions of an energy, and is usually measured in electron volts (ev). The total probability for disintegration of the compound nucleus is proportional to the total width, Γ, which is the sum of the partial widths for all processes which are energetically possible.

In the capture of slow neutrons by nuclei, relatively few reaction types are energetically possible. Types which are always possible are the emission of another neutron (scattering) or of a gamma-ray (n,γ). In some of the light elements, a proton may be emitted (N^{14}), while in others it is possible for the excited compound nucleus to emit an α-particle (B^{10} and Li^6). In some of the heaviest elements (U^{235} and Pu^{239}) the excited compound nucleus may undergo fission. The process of particle emission should predominate whenever it is energetically favorable. However, because an emitted charged particle must penetrate the potential barrier of the nucleus, (n,p) and (n,α) reactions are observed only in the light elements. For most nuclei the only processes observed with slow neutrons are scattering (n,n) and radiative-capture (n,γ) reactions.

When a neutron is captured by a nucleus, the resulting compound nucleus is excited by an amount equal to the binding energy of the neutron in the compound nucleus plus the kinetic energy of the neutron. The value of the cross section for a particular reaction at a given neutron energy is determined by the proximity of this excitation energy to the energy values of one or more of the levels of the compound nucleus, and also by the relative values of the partial widths for the possible reactions. When only one energy level is involved, the cross section is given by the one-level Breit-Wigner formula

$$\sigma(n,x)=\pi\lambda\!\!\!^{-2}f\frac{\Gamma_n\Gamma_x}{(E-E_0)^2+\Gamma^2/4},^{**}$$

where $\lambda\!\!\!^{-}=$the neutron wave-length$/2\pi$, $E_0=$the neutron energy at which the total excitation energy is equal to the energy difference between the energy level and the ground state of the compound nucleus, $E=$the energy of the impinging neutron. Resonances occur when $E=E_0$.

Resonance effects are adequately described by the one-level formula in the immediate neighborhood of a given level, or in the event that neighboring levels are separated by an energy very much greater than the total widths of the resonances. When the level widths are comparable to the level separations, the neutron cross section cannot be obtained by a simple superposition of the resonances; interference effects be-

[39] G. Breit, Phys. Rev. **58**, 506 (1940).
[40] G. Breit, Phys. Rev. **69**, 472 (1946).
[41] G. Breit and E. P. Wigner, Phys. Rev. **49**, 519 (1936).
[42] H. Feshbach, D. C. Peaslee, and V. F. Weisskopf, Phys. Rev. **71**, 145 (1947).
[43] P. L. Kapur and R. Peierls, Proc. Roy. Soc. **A166**, 277 (1938).
[44] A. J. F. Siegert, Phys. Rev. **56**, 750 (1939).
[45] E. P. Wigner, Phys. Rev. **70**, 15, 606 (1946).

** The weighting factor, f, arises from consideration of the spins of the nucleus and neutron, and is given by the expression

$$f=(2J+1)/[(2i+1)(2s+1)],$$

where $s=\frac{1}{2}$ is the spin of the neutron, i is the spin of the target nucleus, and J, the spin of the compound nucleus, can take on the values $|i+j|$, $|i+j-1|$, $\cdots$, $|i-j|$; j has the possible values $l\pm\frac{1}{2}$, where l is the spin imparted to the compound nucleus by the orbital angular momentum of the neutron with respect to the target nucleus. In the low energy region under consideration, $s=\frac{1}{2}$, $l=0$, $J=i\pm\frac{1}{2}$, and $f=\frac{1}{2}[1\pm1/(2i+1)]$, which for large i reduces to $f\cong\frac{1}{2}$. In the evaluation of resonance data in the low energy region (where $\Gamma_\gamma\gg\Gamma_n$) the factor f has usually been included in Γ_n, the neutron width.

tween levels, both constructive and destructive, come into play. These effects have been discussed by a number of authors.[1, 8, 39, 43, 44]

A given neutron resonance can involve either one or more of the various possible reactions [(n,n), (n,γ), (n,p), (n,α), etc.], depending on the relative values of the partial widths. Usually, one or another of the widths predominates, and the resonance observed involves primarily a single reaction. Although the discussion of all resonances proceeds along similar lines, we shall, for convenience, confine our further considerations of resonances to processes in which Γ_γ and Γ_n are the only appreciable partial widths.

The gamma-emission width, Γ_γ, is essentially independent of the energy of the impinging neutron, since the energy available for gamma-ray emission is large (the neutron binding energies vary between 5 and 8 Mev for most nuclei) compared to the variations of slow neutron energy (0–10 kev) for which this discussion is intended. For the resonances which have been experimentally investigated, the values of Γ_γ are about 0.1 ev, with a variation by a factor of 10 in either direction.

The neutron width Γ_n, on the other hand, depends on the neutron energy, increasing as the square root of the neutron energy. For nuclei of atomic weight between 100 and 200 and resonances occurring at a neutron energy of ~ 1 ev, the neutron widths so far measured fall in the range 10^{-4}–10^{-2} ev. In such resonances, the total cross sections correspond mainly to an (n,γ) process, since $\Gamma_\gamma \gg \Gamma_n$, and $\sigma(n,\gamma)/\sigma(n,n) = \Gamma_\gamma/\Gamma_n$. Typical examples of such (n,γ) resonances are the In resonance at 1.44 ev, the Rh resonance at 1.3 ev, and the Ag resonance at 5.1 ev.

Recent work has revealed a number of apparently broad resonances for nuclei of atomic weight $A < 100$ in the region 100–1000 ev. In at least one case (the Mn resonance at ~ 300 ev) the cross section in the resonance has been shown to involve mainly the (n,n) process (scattering), with a peak cross section of $\sim \pi\lambda\!\!\!^{-2}$.[46] For such resonances, $\Gamma_n > \Gamma_\gamma$.

It is expected that the neutron width, Γ_n, in different elements and at a given neutron energy, will depend on the average distance between nuclear energy levels, the width increasing with increased level spacing.[42] According to the Bohr model, for a given excitation energy, the lighter the element, the greater the level spacing. Also, for a given nucleus, the less the excitation energy, the greater the average level spacing. From an examination of the curves in this compilation, one can estimate that the average level spacing in heavy elements ($A > 100$) is $\sim 10-30$ ev; for Al ($A = 28$) the average spacing is ~ 50 kev.[47] These observations suffice to explain many of the data. Thus, resonances are seldom found in light elements, since for an average level spacing of ~ 10 kev, the probability of finding a resonance between 0 and 1 kev (the region which has been adequately investigated) is quite small. When resonances do occur in light elements, they are broad, scattering resonances (for example, Mn and Co).

The failure of resonances to appear in such heavy elements as Sn, Pb, and Bi may be due to an anomalously small binding energy for the neutron captured by these elements.

For scattering resonances, theory[42, 45] predicts an asymmetry in the shape of the resonance. This asymmetry arises from the interference between the constant potential scattering and the resonance scattering, which changes phase by 180° on going through the resonance peak. Thus, according to one of these theories,[42] the cross section should dip to a value lower than the potential scattering cross section on the low energy tail (destructive interference) and maintain a higher value on the high energy tail (constructive interference) of the resonance. The few scattering resonances so far observed have not been measured carefully enough to test this prediction.

For a single (n,γ) resonance, the cross section at the peak ($E = E_0$) will be

$$\sigma_0(n,\gamma) = 4\pi\lambda\!\!\!^{-2} f(\Gamma_n\Gamma_\gamma/\Gamma^2).$$

$\sigma_0(n,\gamma)$ has a maximum, for $\Gamma_n = \Gamma_\gamma$, equal to $\pi\lambda\!\!\!^{-2} f$; in this case, the total cross section would be $2\pi\lambda\!\!\!^{-2} f$. In most (n,γ) resonances, $\Gamma_n \ll \Gamma_\gamma$, $\Gamma \cong \Gamma_\gamma$, and the maximum (total) cross section is

$$4\pi\lambda\!\!\!^{-2} f(\Gamma_n/\Gamma_\gamma).$$

[46] F. G. P. Seidl, S. P. Harris, and A. S. Langsdorf, Jr., Phys. Rev. **72**, 168 (1947).

[47] L. W. Seagondollar and H. H. Barschall, Phys. Rev. **72**, 439 (1947).

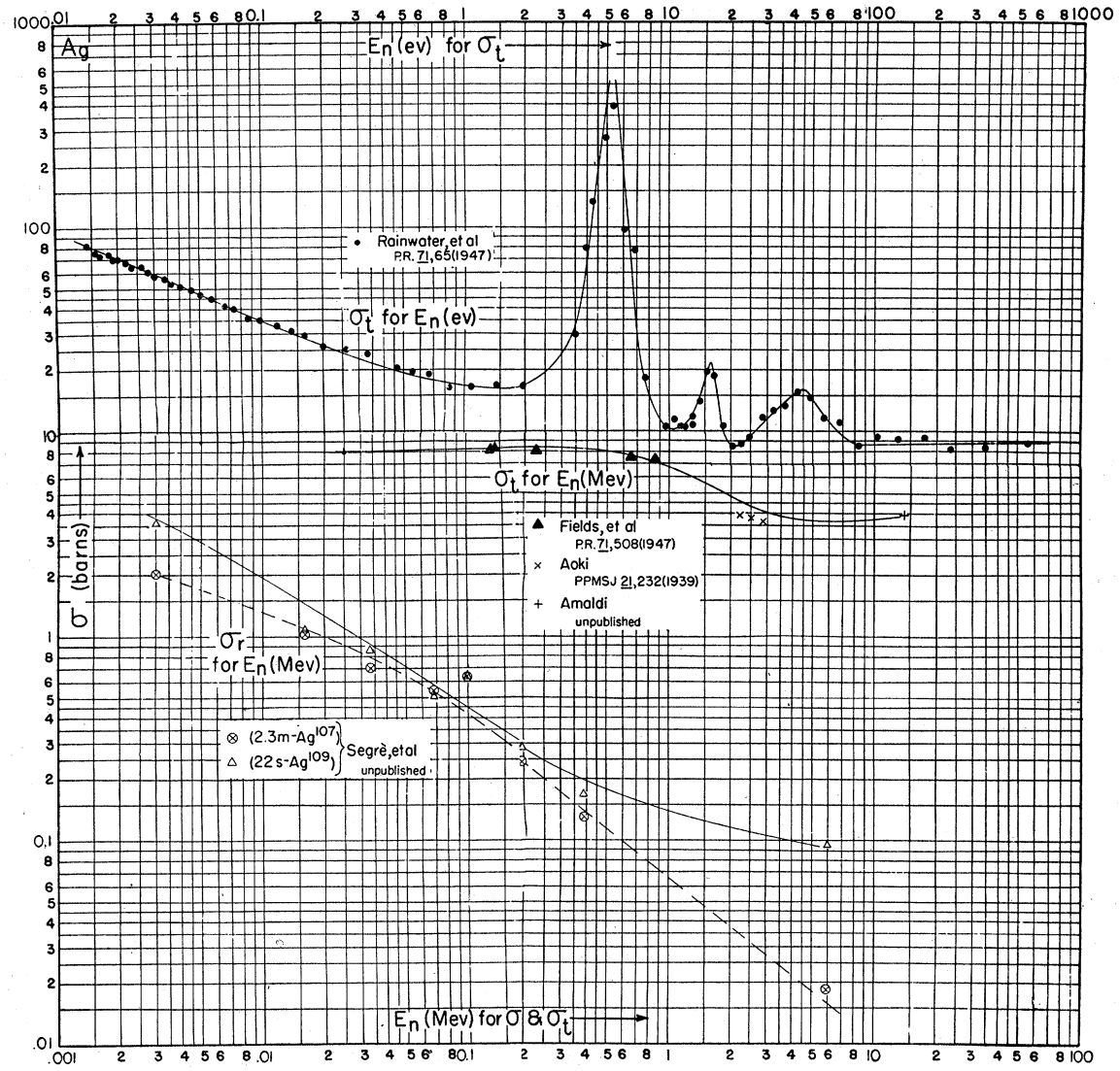

FIG. 45.

At low energies this maximum cross section is quite enormous, as may be seen from the fact that an energy of 1 ev,

$$\pi\lambda\!\!\!^{-2} = \hbar^2/2ME = 6.7\times10^{-19}\ \text{cm}^2 = 0.67\times10^{6}\ \text{barns}.$$

In theory, all of the constants of the resonance could be obtained by a measurement of the maximum cross section and the total width (at half-maximum) of the resonance. In practice, however, a transmission experiment, which measures the total cross section, is seldom sufficient to obtain these quantities with requisite accuracy when the resonance occurs at a neutron energy greater than ~1 ev. By combining transmission data, self-absorption measurements (to obtain σ_0) and an accurate measurement of the thermal neutron ($E\cong 1/40$ ev) cross section

$$\sigma_{th}(n,\gamma) = \pi\lambda\!\!\!^{-}_{th}{}^2 f(\Gamma n_{th}\Gamma_\gamma/E_0^2) \quad (\text{for } E_0 \gg \Gamma, E_{th}),$$

it is possible to evaluate the constants of a given, single resonance.[1, 5–7]

For scattering (n,n) resonances, arising out of the condition $\Gamma_n \gg \Gamma_\gamma$, the maximum cross section is always $\sigma_0(n,n) = 4\pi\lambda\!\!\!^{-2} f$.

In the curves herein reproduced, only those in the region below a few ev are well resolved, since

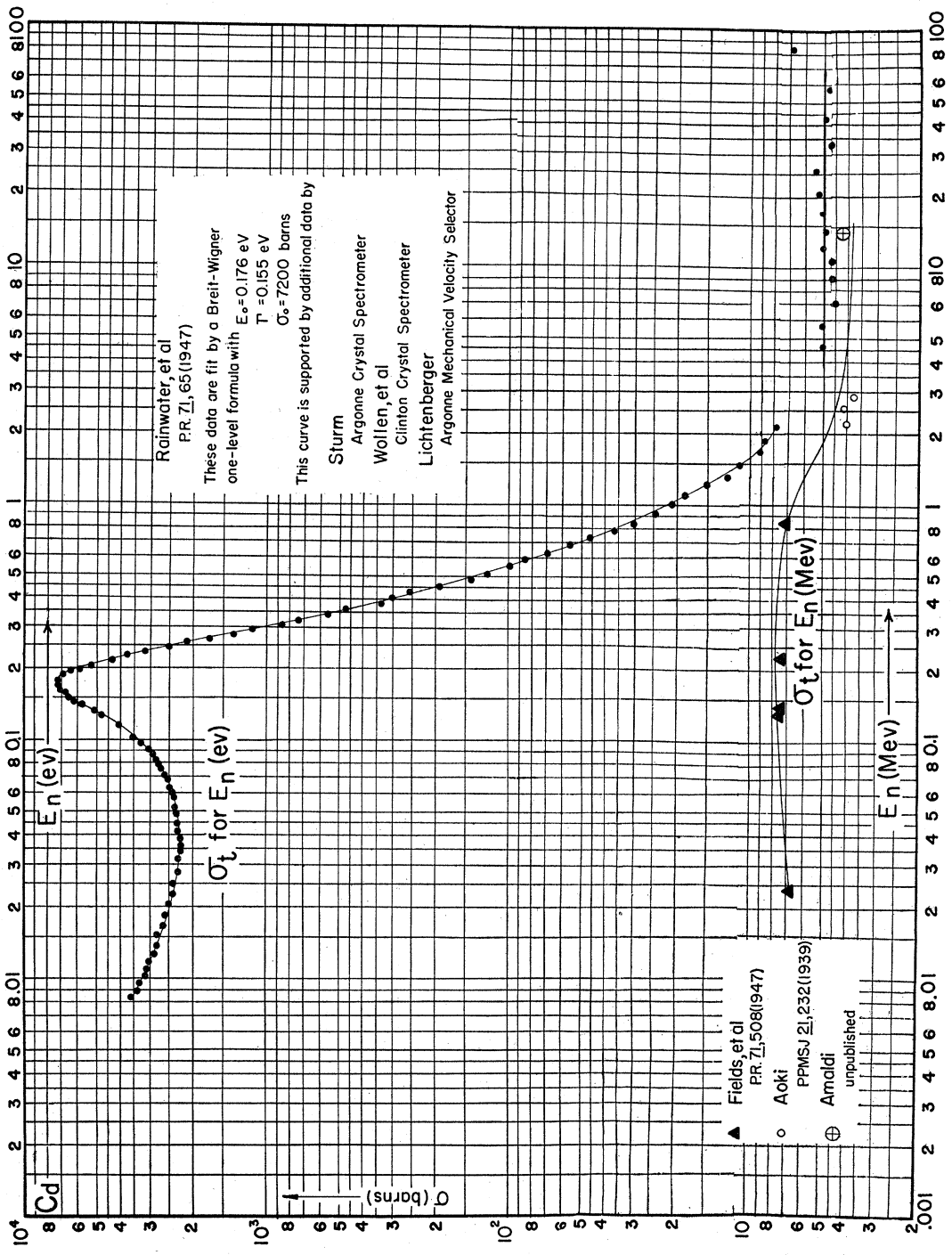

FIG. 46. (See "Note added in proof.")

it is only in this region that the resolution widths of the velocity selectors are smaller than the expected widths of the resonances. As the energy of the neutrons increases beyond a few ev, the resolution of the instruments become appreciably worse, so that measurements in this region merely represent average cross sections over an energy spread at least as great as the width of the resonance under investigation. Consequently, the maximum observed cross sections are very much smaller than the actual cross sections at the peak of the resonance. Furthermore, what

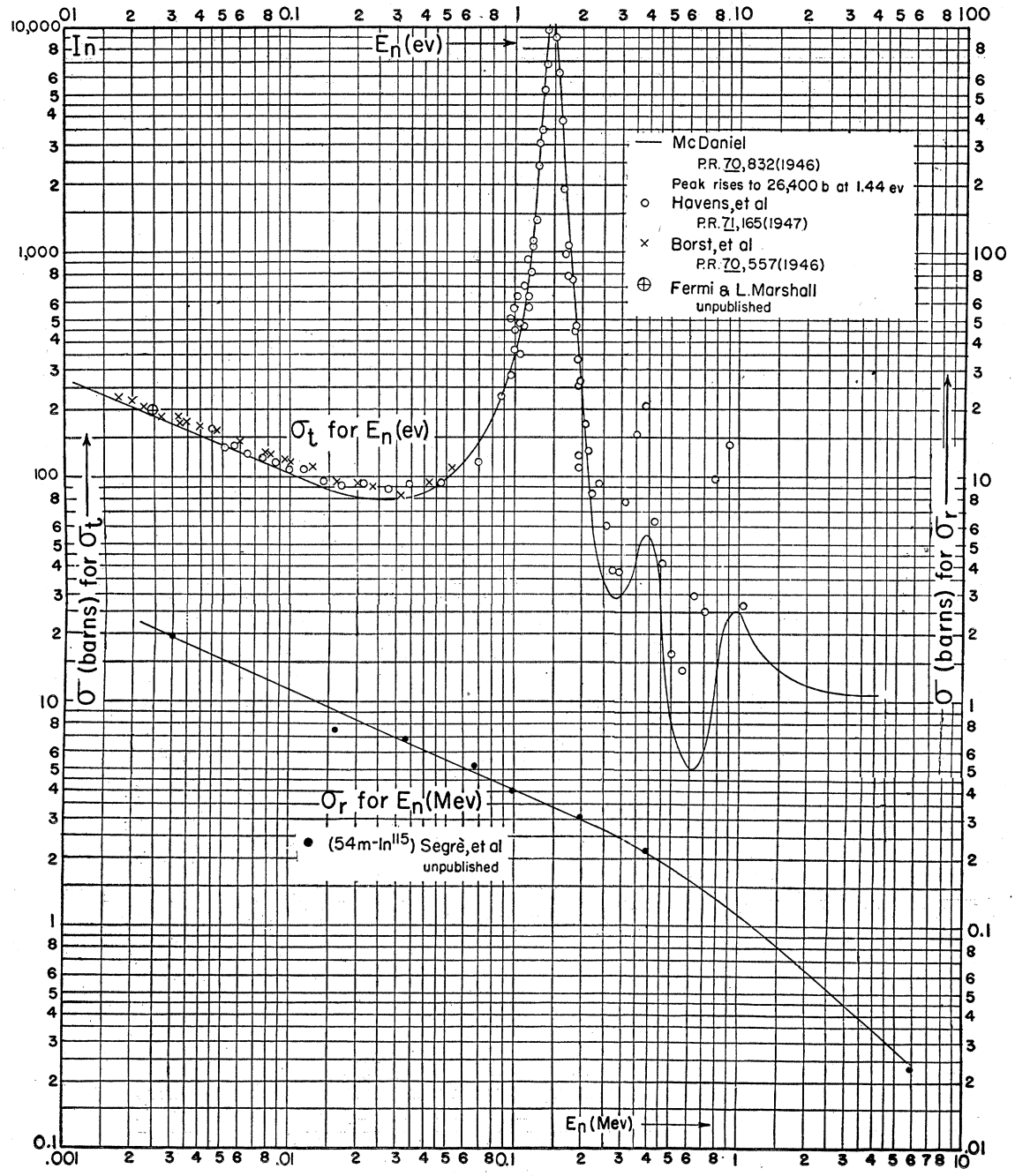

FIG. 47.

often appears to be a broad resonance may turn out, on more careful observation, to be a superposition of two or more adjacent resonances (as in the case of the 35-ev resonance in I).

The compilers are acutely conscious of the dubious validity of drawing solid curves of cross section *vs.* energy through points measured in the neighborhood of a resonance, when the resolution width of the measuring instrument exceeds the expected width of the resonance. Nevertheless, because of the nuclear physicist's interest in the variation of cross section with neutron energy, we have drawn such curves to serve as a visual aid in following those trends in this

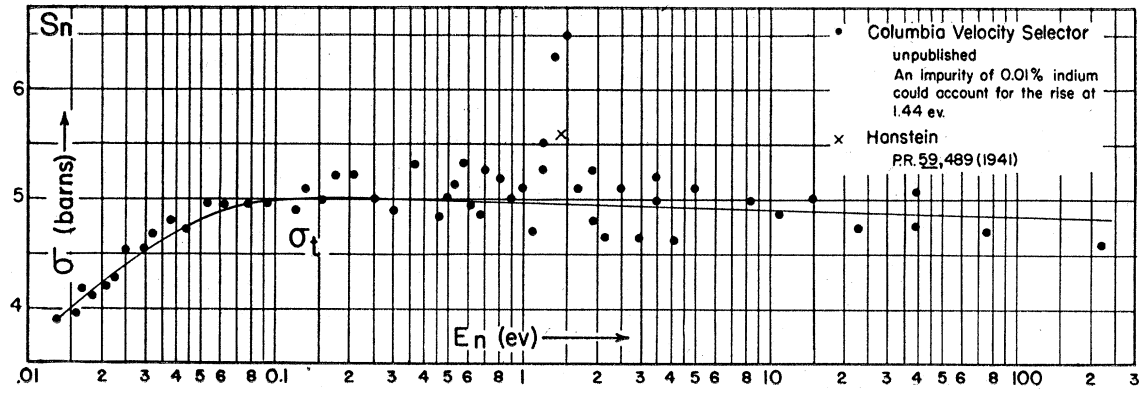

FIG. 48.

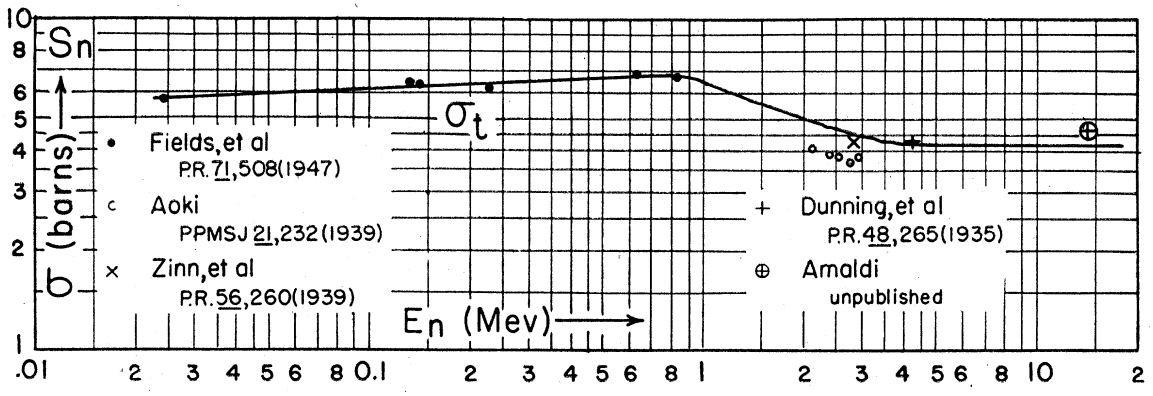

FIG. 49.

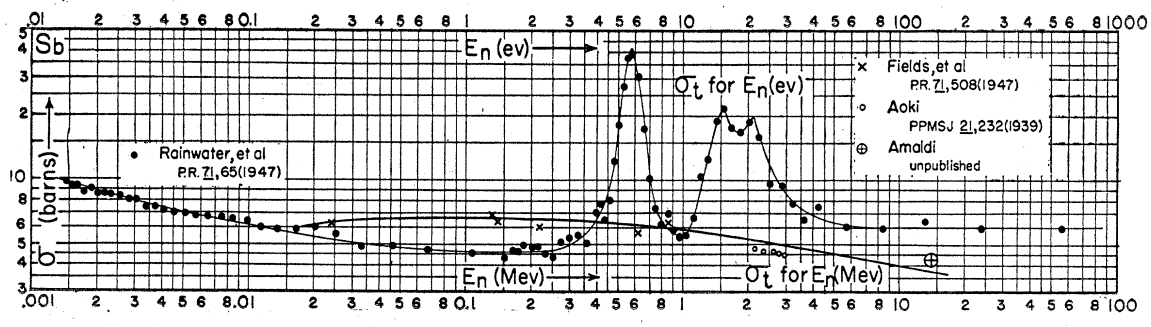

FIG. 50.

variation which are indicated at the present writing.

The usual procedure of the workers in the low energy field is to indicate the resolution width of their instrument by a few triangles placed on the experimental curve at various energies. Instead of following this procedure, we have compiled Table I which provides an estimate of the resolution widths of the monochrometers now being used.

The phenomena arising in the thermal neutron region (0−0.1 ev) are of sufficient interest to merit separate consideration. The cross section in this region is strongly dependent on the position of the nearest resonance. When an (n,γ) resonance occurs in, or very close to, the thermal region (as in Cd), the cross section throughout this region is very large—of the order of 10^4 barns and greater. The cross-section curves, for elements having a resonance in this region, do not show the characteristic narrow, sharp resonance peak, since the 1/v factor prevents the falling-off on the low energy side of E_0. Hence, any of these substances can be used as neutron filters for all energies up to $\sim E_0$.

Radiative-capture resonances close to, but above, the thermal region (1–10 ev) lead to high thermal neutron-capture cross sections, which decrease with increasing neutron velocity according to the 1/v law (see the curves for In, Rh, Ag, Au).

Deviations from the 1/v law for thermal neutron capture are frequently observed, and they can be explained by taking into account the effects of resonances occurring between 0.1 and 1 ev (Ir and Eu), or at negative energies, i.e., an energy level of the compound nucleus occuring at an energy slightly less than the binding energy of the captured neutron (Hg and Eu).

If the lowest resonance occurs far above the thermal region (Eo>10 ev), the capture cross section in the thermal region is small. The total cross section should consist of a superposition of an essentially constant nuclear scattering cross section (the value of this varies from element to element in the range 1–20 barns), and this small capture cross section, varying as 1/v. This pattern is, however, seldom observed in the region below ~0.1 ev. Instead, the cross section in this region behaves in an erratic fashion (see curves for Pb, Ge, Al, O, C, Be). This behavior is due to "crystal" or interference effects, arising from the coherent scattering of neutrons whose wave-length is of the order of or greater than the distance between the atoms in the molecule or crystal.[1,48] Much useful information, relating to the structure of crystals and polycrystalline materials can be obtained from studies of these interference effects.[31,49,50] Furthermore, the study of these interference effects yields information on details of nuclear scattering, such as the phase of the scattered wave,[50–52] the dependence of the scattering cross section on nuclear spin,[53] and the effects of magnetic fields on the neutron scattering process.[54,55]

TABLE I. Resolution widths of various monochrometers.

Monochrometer	Useful energy range	Resolution 0.025 ev	0.1 ev	1 ev	10 ev	100 ev
Mechanical	0.004–0.2 ev	0.005 ev	0.1 ev	—	—	—
Crystal	0.02 –50 ev	0.001 ev	0.05 ev	0.5 ev	10 ev	—
Modulated source	0.001–10,000 ev	0.001 ev	0.05 ev	0.1 ev	1 ev	20 ev

In the region of intermediate neutron energies (1 kev to 1 Mev) the picture of a series of single, separated resonances—valid for cross-section data in the low energy region—is no longer applicable. Although, for the light elements, the cross section continues to show sharp resonance phenomena (C, N, O, Al), the levels in heavier elements first overlap and finally merge into a continuum, the total cross section becoming essentially constant. Furthermore, although at the lower end of the intermediate energy region the wave-length of the neutron is large compared to the nuclear radius, as the energies approach 1 Mev the wave-length becomes comparable to, and finally smaller than the nuclear radius (except in the light elements); when this occurs, the simple Breit-Wigner picture is no longer applicable.

In the competition between processes resulting

[48] J. H. Van Vleck, University of Pennsylvania Bicentenial Conference 1941, p. 51.
[49] E. Fermi, W. J. Sturm, and R. G. Sachs, Phys. Rev. **71**, 589 (1947).
[50] M. L. Goldberger and F. Seitz, Phys. Rev. **71**, 294 (1947).
[51] E. Fermi and L. W. Marshall, Phys. Rev. **71**, 666 (1947).
[52] E. Fermi and W. H. Zinn, Phys. Rev. **70**, 103 (1946).
[53] J. S. Schwinger and E. Teller, Phys. Rev. **52**, 286 (1937).
[54] O. Halpern, M. Hamermesh, and M. H. Johnson, Phys. Rev. **59**, 981 (1941).
[55] J. S. Schwinger, Phys. Rev. **51**, 544 (1937).

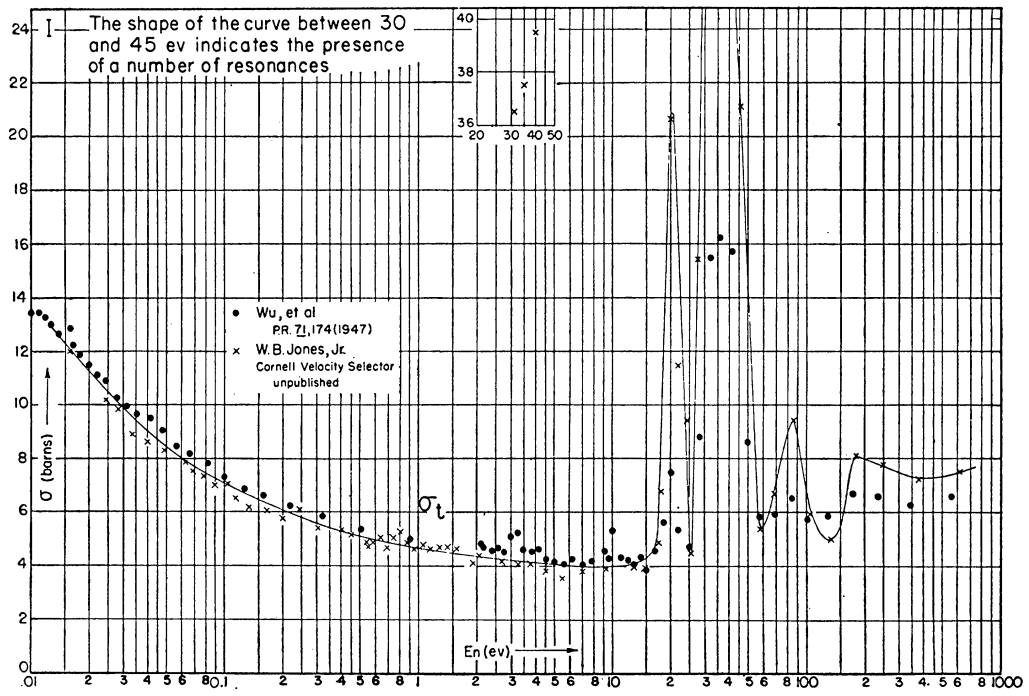

FIG. 51. (See "Note added in proof.")

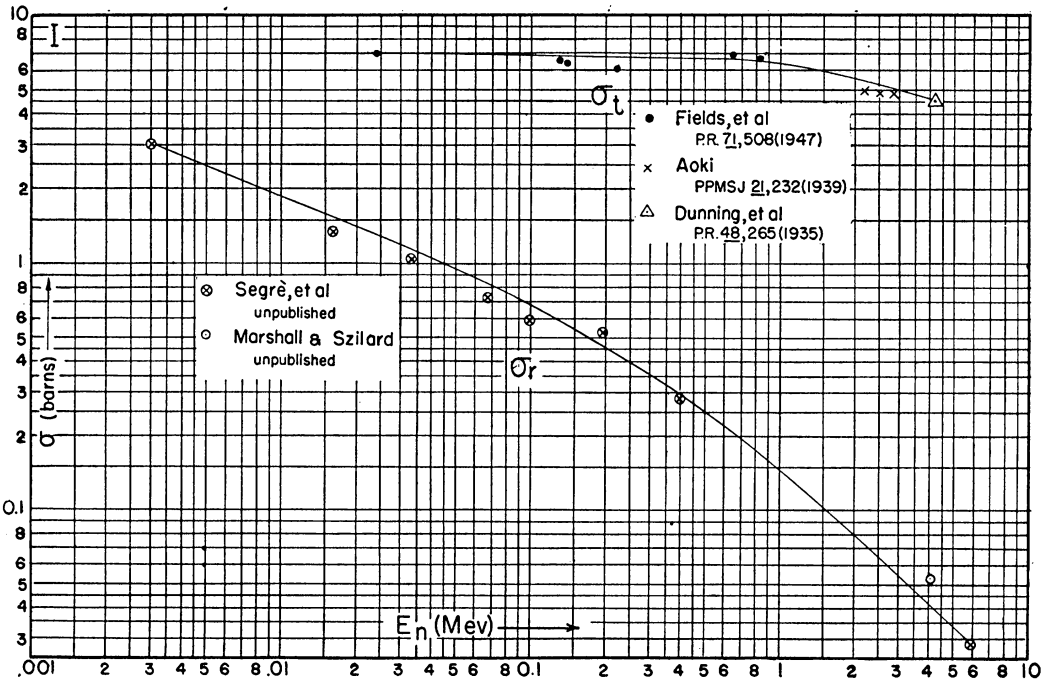

FIG. 52.

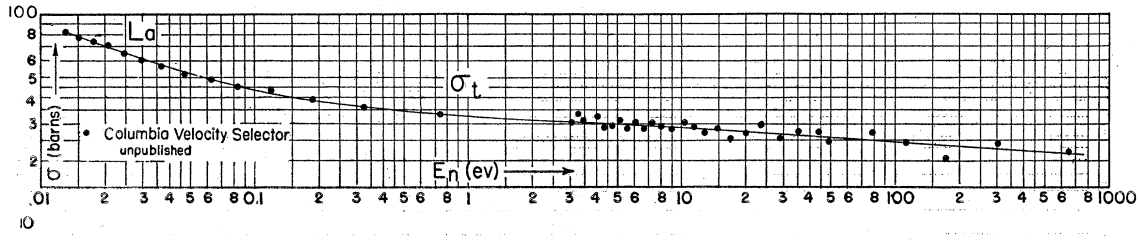
La
σ_t
Columbia Velocity Selector
unpublished
σ (barns)
E_n (ev)

FIG. 53.

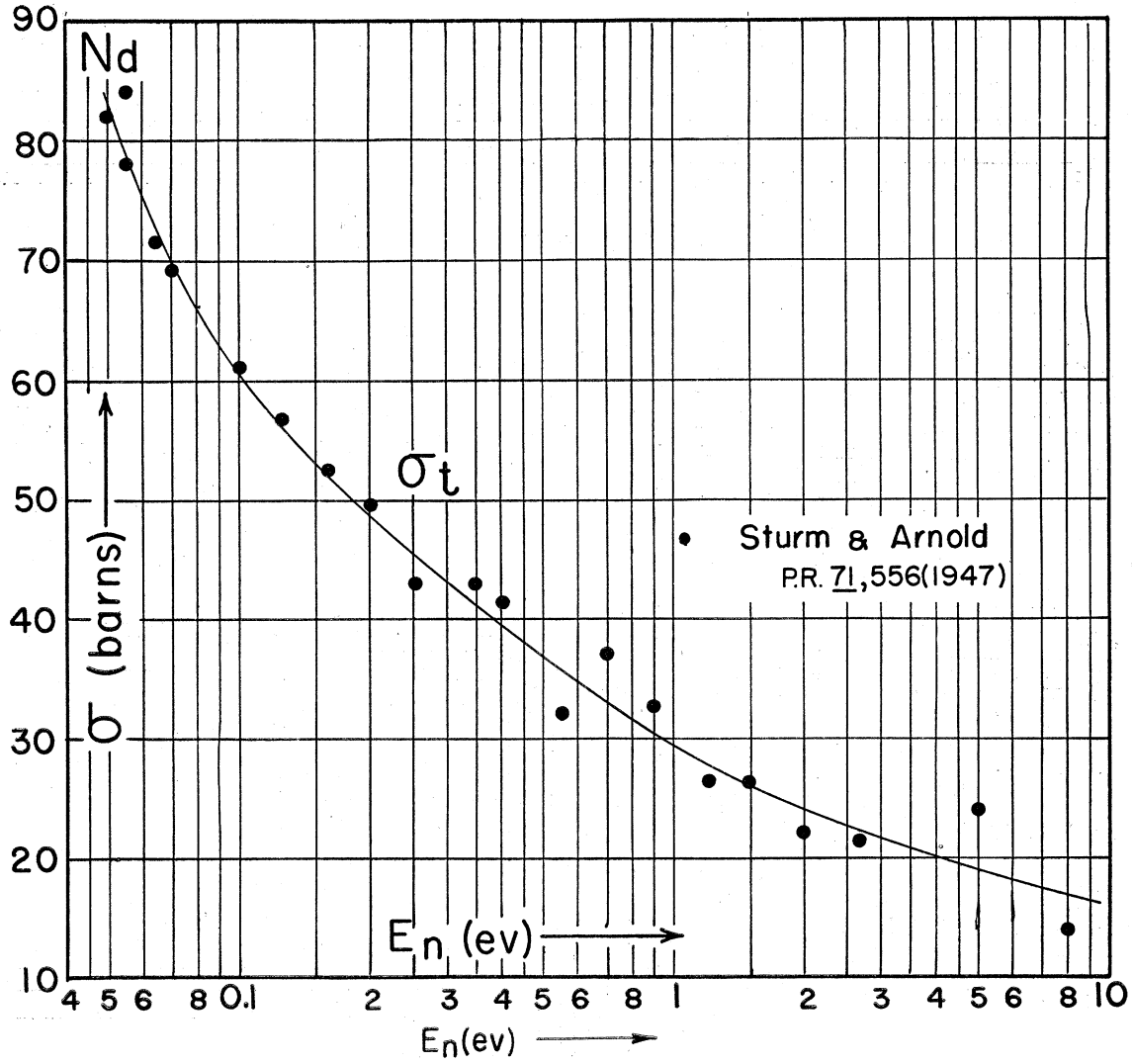
Nd
σ_t
Sturm & Arnold
P.R. 71, 556(1947)
σ (barns)
E_n (ev)
E_n(ev)

FIG. 54.

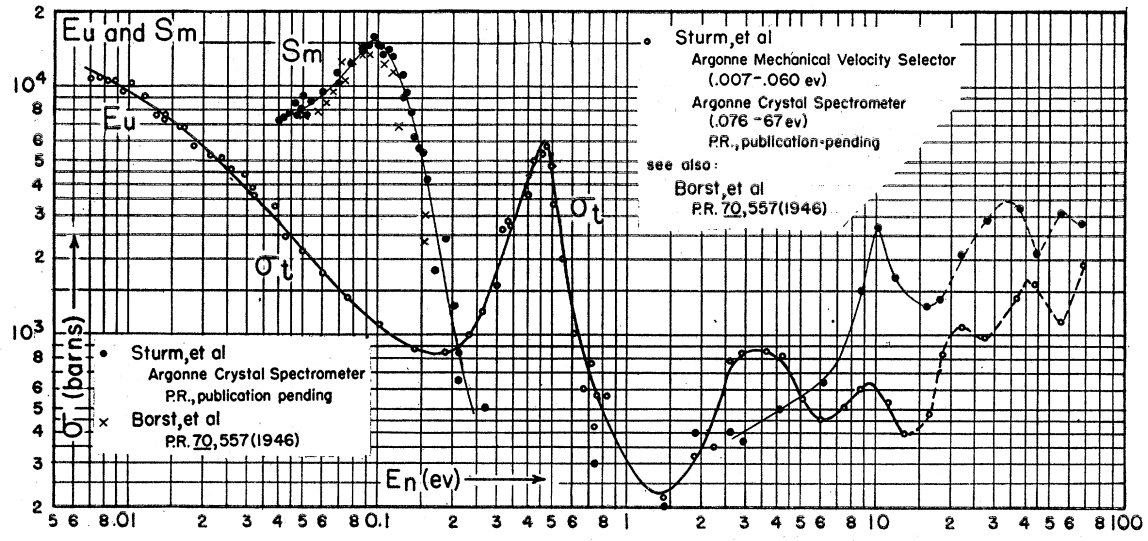

FIG. 55. (See "Note added in proof.")

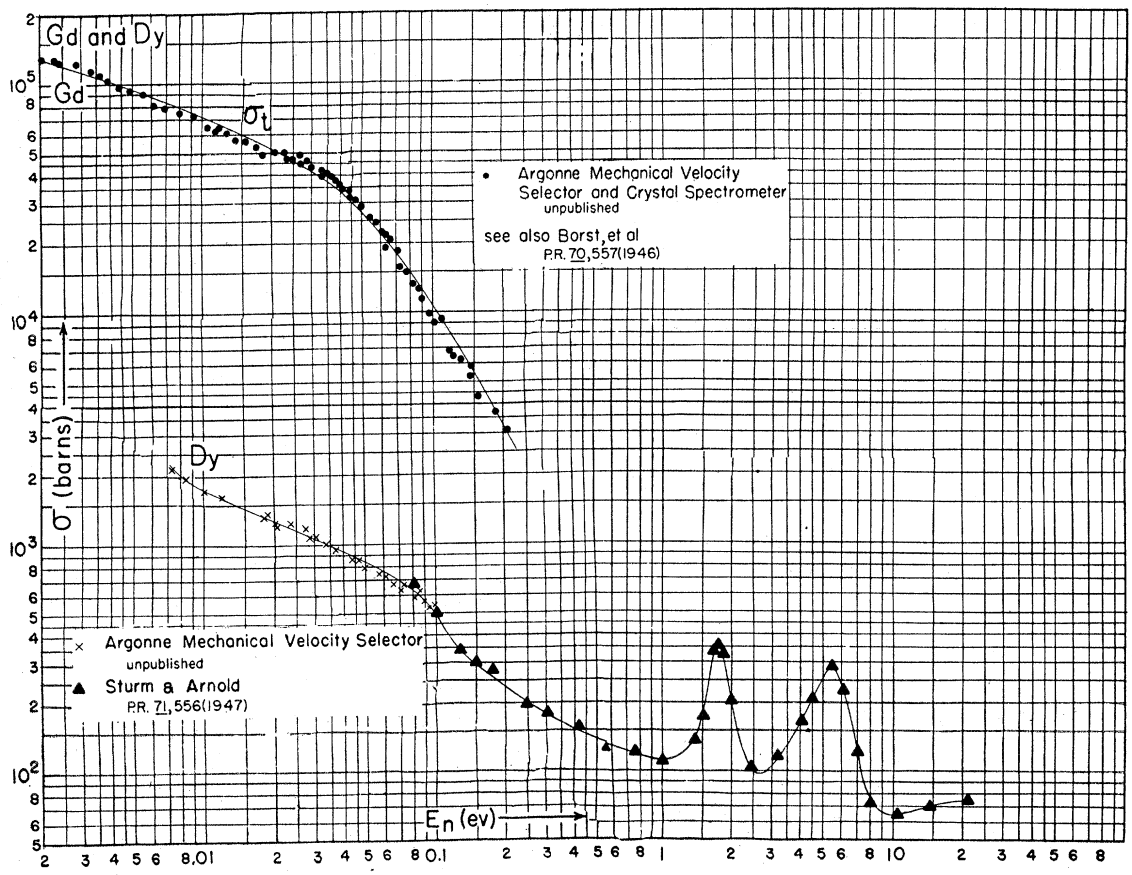

FIG. 56. (See "Note added in proof.")

from neutrons of intermediate energies, scattering predominates, since the neutron width (which increases as $E^{\frac{1}{2}}$) is larger than the other widths in this region. For light elements, in which the levels are still separate, the peak cross sections should decrease with the neutron energy ($\pi\lambda^2$ varies from 670 barns at 1 kev to 0.67 barns at 1 Mev).

In the light elements, radiative capture cross sections—already small in the low energy region ($<10^{-24}$ cm^2)—become very small ($<10^{-26}$ cm^2) at intermediate energies. Other reactions, such as (n,p) and (n,α), exhibit much larger cross-section values, although the cross sections for these seldom exceed $\sim$0.1 barn. The exceptional cases of the highly exothermic (n,α) reactions in Li^6 and B^{10} (which follow a 1/v law up to $\sim$1 kev) possess cross sections of a few barns in this energy range. In a number of light elements (n,p) and (n,α) reactions, which are energetically impossible in the low energy region, become possible in this region; the cross sections for these show a typical threshold character because of the emerging particle's increasing penetration of the potential barrier with increasing neutron energy (see the S and P (n,p) cross sections). A few resonances for (n,p) and (n,α) reactions have been observed in the intermediate energy region (N^{14}, B^{10}, Li^6).

For the elements in which the levels merge into a continuum (elements of $A>100$, with the possible exception of such anomalies as Sn, Pb, and Bi) the total cross sections, which are mainly due to scattering, remain essentially constant. The radiative capture cross sections, although small, are still appreciable, having values up to a few barns in some elements (In and Au). Heavy-particle reactions, like (n,p) and (n,α), no longer appear, because of the impenetrability of the potential barrier. In some of the heaviest elements (see Np^{237}) in which thermal neutron fission is energetically impossible, fission may take place at intermediate neutron energies; the fission cross section exhibits a typical threshold-reaction behavior.

As we approach the upper end of the intermediate energy range, inelastic scattering of neutrons begins to appear among the possible reactions for heavy elements; inelastic scattering is energetically possible when the neutron energy exceeds the energy of the lowest level of the target nucleus. Because of the complex nature of the inelastic scattering process and the strong dependence of the measured cross section on the experimental arrangement (especially on the energy sensitivity of the detector) inelastic scattering measurements are in general not adaptable to graphical representation of cross section *vs.* neutron energy. No inelastic scattering data have been included in this compilation.

The details outlined above do not appear in most of the curves. Even the most recent photoneutron measurements, though applied to a wide range of atomic numbers, suffer from the fact that there are relatively large energy gaps for which there has been found no appropriate neutron source. Furthermore, the homogeneity of these sources is not sufficient to reveal the expected structure in the light elements.

The two neutron sources depending on accelerated particles which have been used to explore this region (Li (p,n) and C (d,n)) have unfortunately been applied to relatively few elements. Some structure is revealed in C, N, and O. What can be expected from the exploitation of present techniques (thin targets, extremely good voltage control, and the use of a threshold (p,n) reaction as in Li) is exemplified by the recent work of Seagondollar and Barschall[47] on the total cross section of Al. The resolution in these measurements ($\sim$10 kev at the low end, $\sim$50 kev at 1 Mev), though not sufficient to give the actual shape and peak cross sections of all the resonances in this region, has revealed the existence of an extensive series of resonances, separated by $\sim$50 kev.

The curves of σ_t *vs.* E for Al illustrate a fact which has been implied in the general discussion at the beginning of this article and which is worth emphasizing at this point. It is now feasible to obtain a continuous picture of neutron cross sections from 0 to 10 Mev. This has been made possible by the extension of slow-neutron velocity selector measurements to $\sim$10 kev and of intermediate neutron measurements, through the Li (p,n) reaction down to $\sim$5 kev. Thus, the techniques of neutron spectroscopy are rapidly being extended and improved, and the gaps in the measurements—so evident in the prewar data—are slowly being filled in.

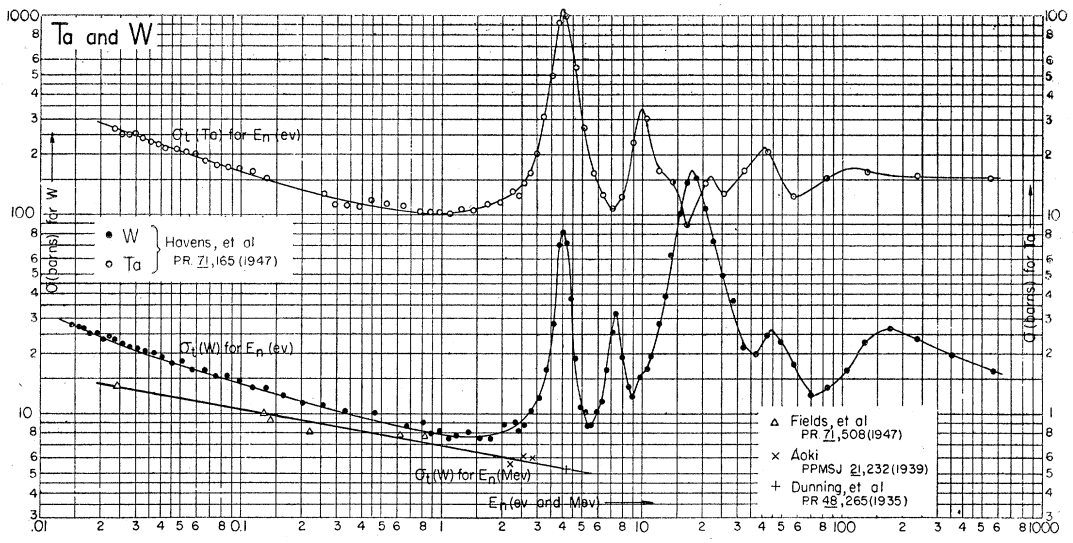

FIG. 57.

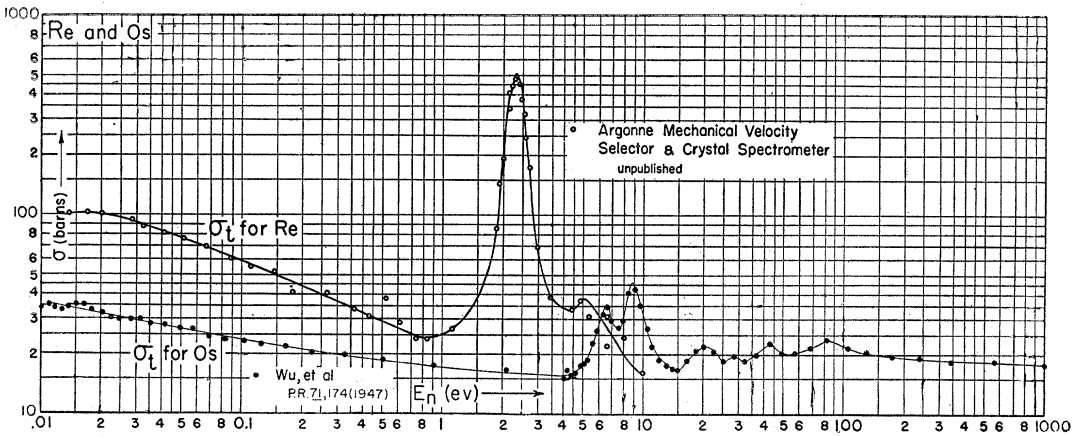

FIG. 58.

For high energy neutrons ($E>1$ Mev), the neutron wave-lengths are smaller than the nuclear radius, R (in all but the very light elements). The total cross sections are now constant, and equal to $2\pi R^2$. Of this, πR^2 represents the capture of the neutron into a compound nucleus and the resultant competition between the alternative processes, of which elastic scattering, inelastic scattering and (at neutron energies exceeding the binding energy of a neutron in the scattering nucleus) $(n,2n)$ reactions are the most important. Radiative-capture cross sections are small, ranging from ~ 0.1 barn for the heaviest elements, to ~ 0.001 barn or less for the lighter elements.[56] More of the (n,p) and (n,α) reactions are now energetically possible; these cross sections attain values of a few tenths of a barn.

The remaining πR^2 in the total cross section represents the process of "shadow scattering" which, when $\lambda\!\!\!^{-} < R$, derives from the diffraction of that portion of the fast neutron beam passing close to the nucleus. This diffraction effect introduces an angular asymmetry in the scattering, since the "shadow scattering" is confined to within small angles of the order of $\lambda\!\!\!^{-}/R$. These

[56] D. J. Hughes, unpublished.

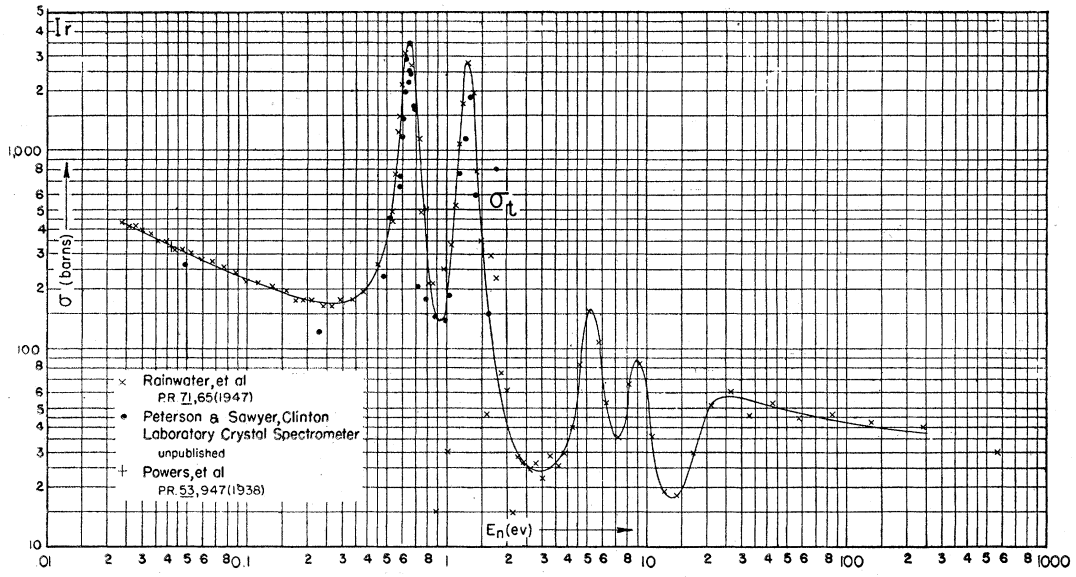

FIG. 59. (See "Note added in proof.")

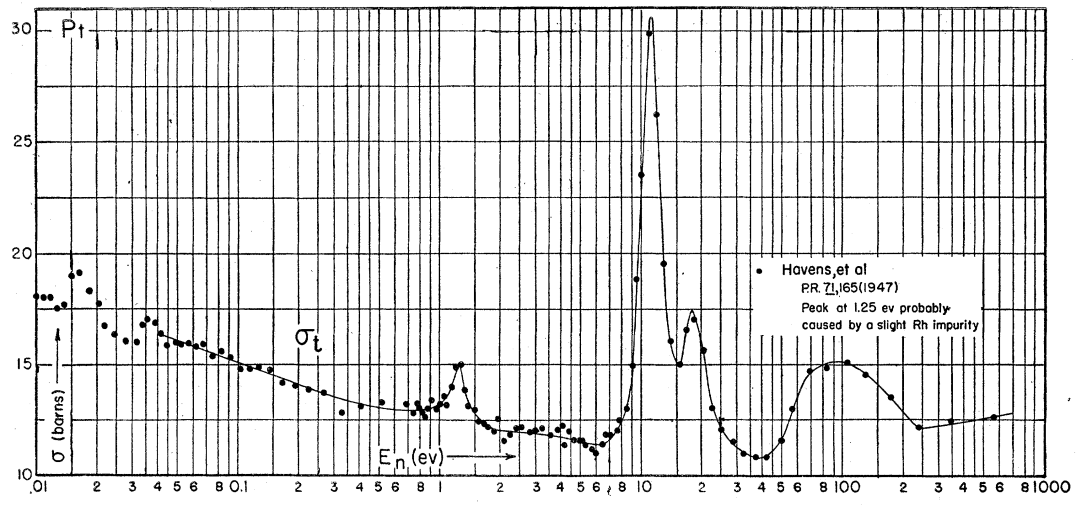

FIG. 60.

effects fall off rapidly as the scattering angle exceeds $\lambda\!\!\!^{-}/R$; in the transition region, at angles close to $\lambda\!\!\!^{-}/R$, interference maxima and minima are expected and have been observed.[57]

While the scattering cross sections for low and intermediate energy neutrons are spherically symmetrical (*S*-wave scattering), the high energy cross sections depart from spherical symmetry, not only because of the small-angle scattering discussed above, but also because the fast neutrons can now change the angular momentum of the target nucleus, introducing the possibility of P, D, etc., wave scattering. It should be emphasized again that the total cross-section curves shown in this compilation (Table II) are mostly derived from transmission experiments, which automatically integrate the cross section over all angles greater than a given small angle, depending on the geometry of the experiment. In some experiments, the angular dependence of

[57] E. Amaldi, D. Bocciarelli, B. N. Cacciapuota, and G. C. Trabacchi, Nuovo Cimento **3**, 203 (1946).

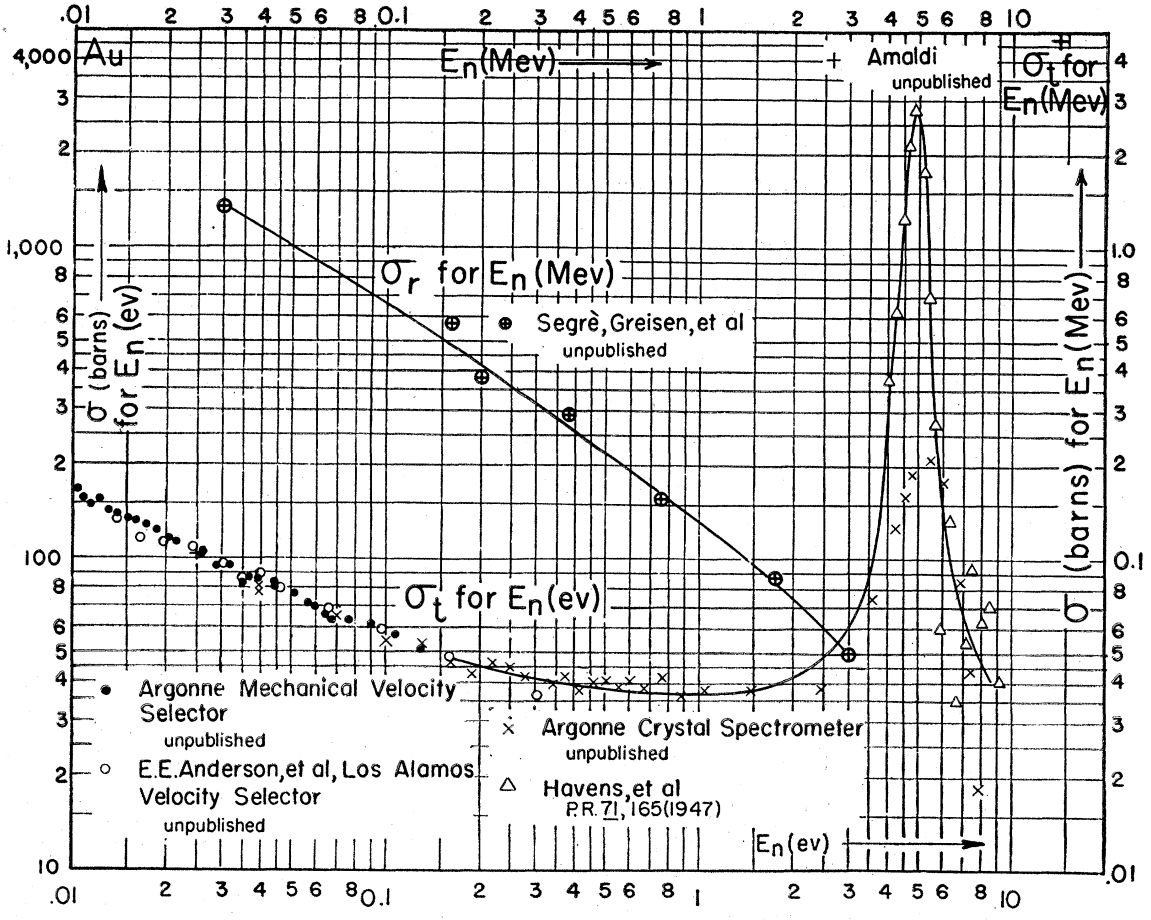

FIG. 61. (See "Note added in proof.")

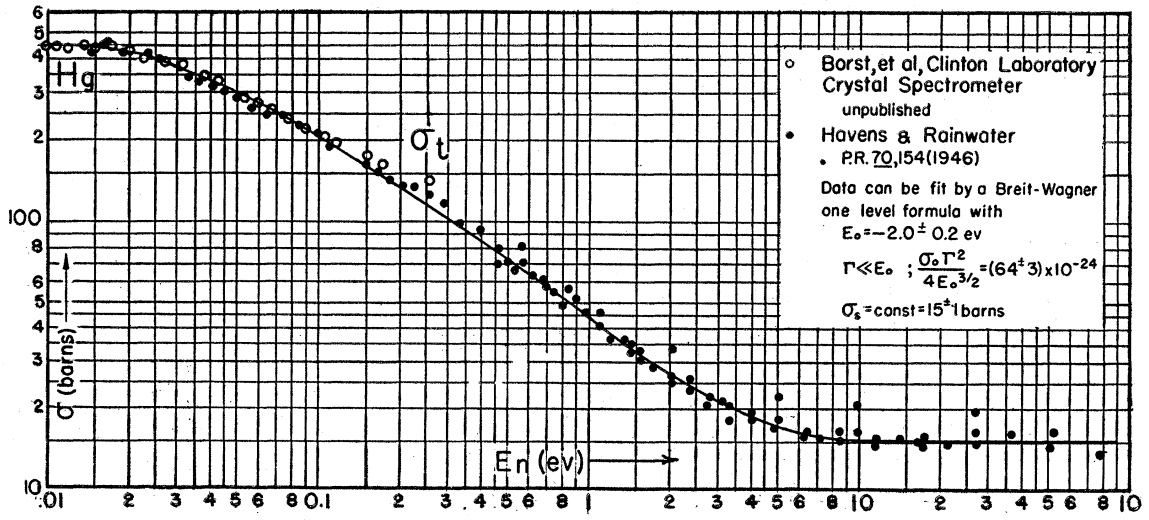

FIG. 62.

the scattering has been measured; such curves are not included in this compilation.

The detailed study of neutron cross sections at high energies has been made possible mainly by the extension of the D(d,n) reaction which, for a given incident deuteron energy and angle, produces neutrons of a single energy. The neutron energy range available from this reaction has been increased to ~6 Mev, and is limited only by the deuteron energies which can be obtained from accurately controlled, high energy, particle accelerators. Thus, the prewar measurements of Aoki,[11] Zinn, *et al.*[13], and MacPhail,[12] using low voltage machines and the D(d,n) reaction to produce neutrons of energy between 2 and 3 Mev, have been extended for a few elements; the prewar measurements are still the only ones for most elements. The energies of the neutrons used by Aoki and by Zinn, *et al.* have been plotted by use of the corrections made by MacPhail for target thickness and from a more accurate knowledge of the D(d,n) reaction energy.

To these measurements below 6 Mev we have added the work of Dunning, *et al.*[3] in which they used the heterogeneous neutron spectrum obtained from Rn+Be sources. These cross sections have been plotted at an energy of 4.2 Mev.

In the region above 10 Mev, use has been made of the Li(d,n) reaction, which is highly exothermic (14.55 Mev) and which, unfortunately, also results in a highly inhomogeneous neutron energy distribution. This disadvantage has been partially offset by the use of various threshold detectors, such as the $Cu^{63}(n,2n)$ reaction with a threshold of ~11 Mev or the $C^{12}(n,2n)$ reaction, threshold ~21 Mev. The first detector was used by Amaldi and coworkers,[57, 58] in experiments in which the average neutron energy was ~14 Mev. The second detector was used by Sherr to obtain the total cross sections of a number of elements at a neutron energy between 20 and 25 Mev.[59, 60] Since the latter could not be conveniently fitted on the curves, they have not been included in this compilation. Points above 15 Mev are included in the exceptional case of hydrogen which, because of its greater theoretical interest, has been more completely investigated in the high energy region than any other element.

The recent development of very high energy (~100 Mev or greater) particle accelerators, opens up the vast possibilities of production of very high energy neutrons, and their use in determining nuclear cross sections. This field is as yet unexploited.

We again wish to express our thanks to the many scientists who without exception have granted us permission to use their unpublished data. We are especially indebted to the Columbia Velocity Selector Group, J. R. Dunning, W. W. Havens, Jr., L. J. Rainwater, and C. S. Wu, who have made available the results of their experiments as soon as these were completed, and who have permitted us to publish a considerable body of data which have not appeared in print. We are similarly indebted to W. J. Sturm for his constant cooperation with regard to the Argonne Laboratory velocity selector results. The cross-section data, due to Amaldi and co-workers, were transmitted to us by E. Amaldi during his recent visit in this country. Some of these data have been published since this compilation was prepared.[57]

We wish to thank R. S. Mulliken and W. H. Zinn for facilitating the publication of Manhattan Project declassified data prior to the publication of the Manhattan Project Technical Series.

Space limitations have prevented explicit reference, on the curves, to all of the workers concerned with particular sets of unpublished data. Toward this end, we include the following:

1. Argonne Crystal Spectrometer Group: G. P. Arnold, W. J. Sturm, S. H. Turkel, and W. H. Zinn.
2. Argonne Mechanical Velocity Selector Group: T. Brill and H. V. Lichtenberger; also E. Fermi, L. W. Marshall, and J. Marshall.
3. Clinton Crystal Spectrometer Group: L. B. Borst, A. J. Ulrich, C. L. Osborne, and B. Hasbrouck; also E. O. Wollan, S. Bernstein, K. C. Peterson, and R. B. Sawyer.
4. Los Alamos Velocity Selector Group: E. E. Anderson, L. S. Lavatelli, B. D. McDaniel, and R. B. Sutton.

[58] M. Ageno, E. Amaldi, D. Bocciarelli, and G. C. Trabacchi, Phys. Rev. **71**, 20 (1947).
[59] R. Sherr, Phys. Rev. **61**, 734 (1942).
[60] R. Sherr, Phys. Rev. **68**, 240 (1945).

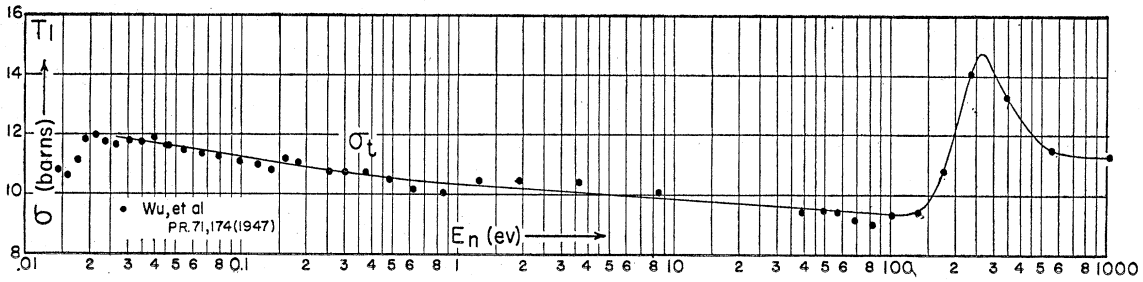

FIG. 63.

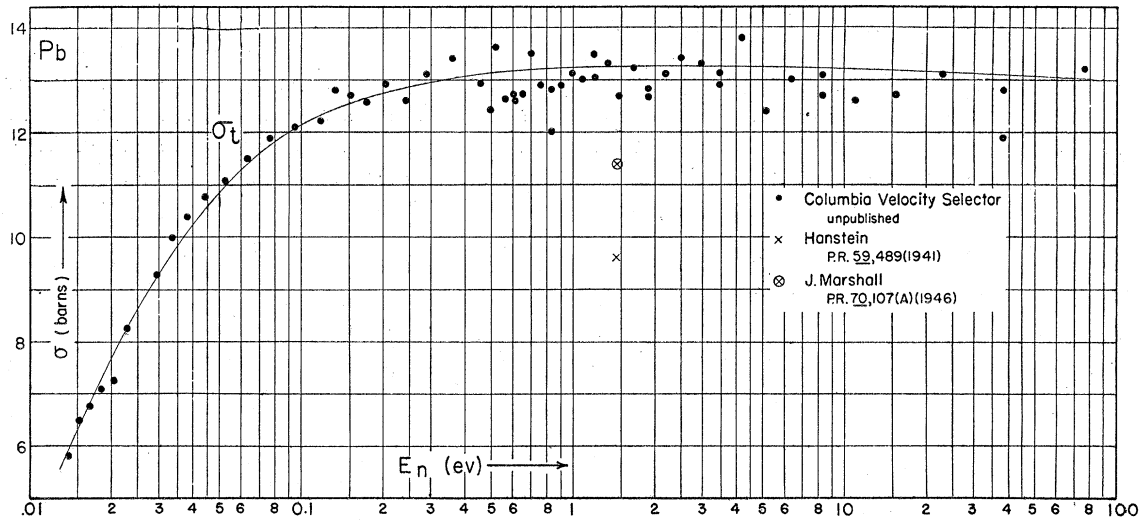

FIG. 64.

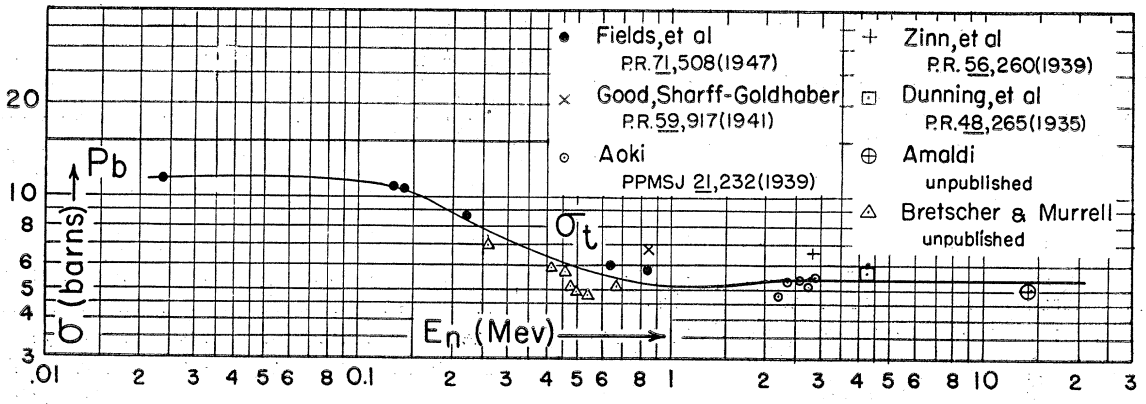

FIG. 65.

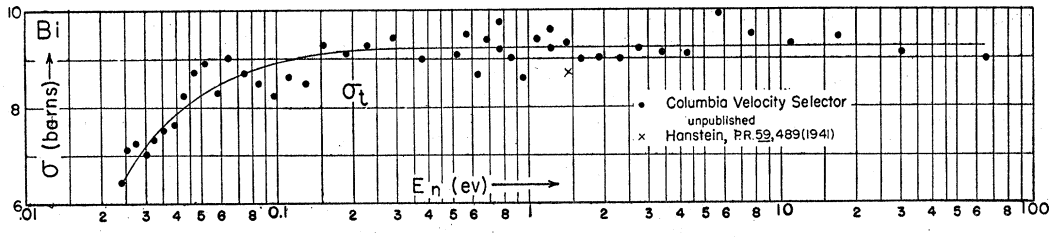

FIG. 66.

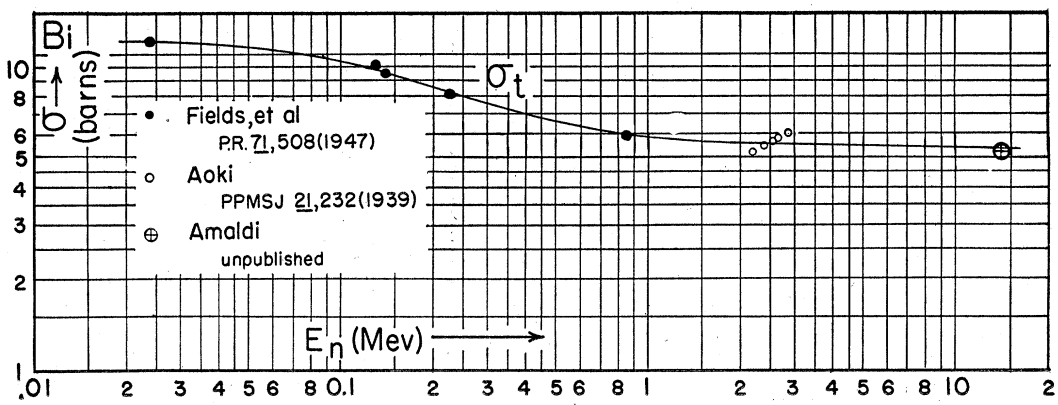

FIG. 67.

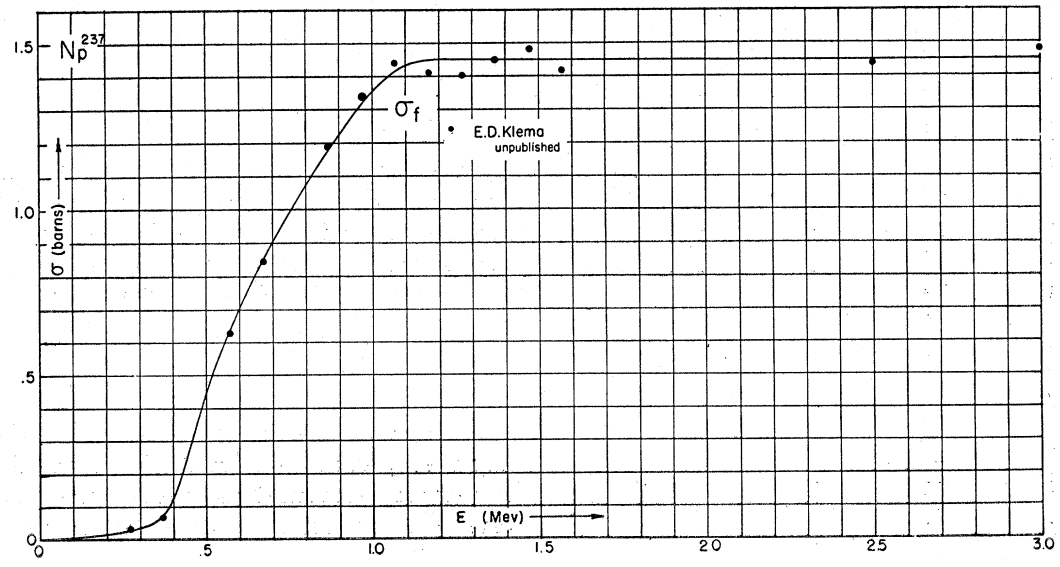

FIG. 68. (See "Note added in proof.")

TABLE II. Table of curves included in this review.

Atomic No.	Element	Low energy	High energy
1	H	σ_t	σ_t
	D	σ_t	σ_t
2	He		σ_s
3	Li	σ_t	σ_α
4	Be	σ_t	σ_t, σ_α
5	B	σ_α	σ_t, σ_α
6	C	σ_t	σ_t
7	N	σ_t	σ_t, σ_s, σ_p, σ_α
8	O	σ_t	σ_t
9	F	σ_t	σ_t
10	Ne		
11	Na		σ_t
12	Mg	σ_t	σ_t
13	Al	σ_t	σ_t
14	Si	σ_t	
15	P	σ_t	σ_t, σ_p
16	S	σ_t	σ_t, σ_p, σ_α
17	Cl	σ_t	
18	A		
19	K		σ_t
20	Ca		
21	Sc		
22	Ti		
23	V		
24	Cr	σ_t	
25	Mn	σ_t	
26	Fe	σ_t	σ_t
27	Co	σ_t	
28	Ni	σ_t	σ_t
29	Cu	σ_t	σ_t
30	Zn	σ_t	σ_t
31	Ga		
32	Ge	σ_t	
33	As		
34	Se		
35	Br		
36	Kr		
37	Rb		
38	Sr		
39	Y		
40	Zr	σ_t	
41	Cb	σ_t	
42	Mo		
43	Tc		
44	Ru	σ_t	
45	Rh	σ_t	
46	Pd		
47	Ag	σ_t	σ_t, σ_r
48	Cd	σ_t	σ_t
49	In	σ_t	σ_r
50	Sn	σ_t	σ_t
51	Sb	σ_t	σ_t
52	Te		
53	I	σ_t	σ_t, σ_r
54	Xe		
55	Cs		
56	Ba		
57	La	σ_t	
58	Ce		
59	Pr		
60	Nd	σ_t	
61	Pm		
62	Sm	σ_t	
63	Eu	σ_t	
64	Gd	σ_t	
65	Tb		
66	Dy	σ_t	
67	Ho		
68	Er		
69	Tm		
70	Yb		
71	Lu		
72	Hf		
73	Ta	σ_t	
74	W	σ_t	σ_t
75	Re	σ_t	
76	Os	σ_t	
77	Ir	σ_t	
78	Pt	σ_t	
79	Au	σ_t	σ_t, σ_r
80	Hg	σ_t	
81	Tl	σ_t	
82	Pb	σ_t	σ_t
83	Bi	σ_t	σ_t
84	Po		
85	At		
86	Rn		
87	Fr		
88	Ra		
89	Ac		
90	Th		
91	Pa		
92	U		
93	Np		σ_f
94	Pu		
95	Am		
96	Cm		

TABLE II. (*Continued*).

5. Los Alamos Linear Accelerator Group: C. L. Bailey, W. E. Bennett, T. Bergstralh, J. M. Blair, D. H. Frisch, A. O. Hanson, J. L. McKibben, R. D. Perry, H. T. Richards, and J. H. Williams.
6. Los Alamos Radioactive Sources Group: M. Deutsch, G. A. Linenberger, T. A. Miskel, and E. Segrè; also (for σ_r of Au) K. I. Greisen and J. H. Williams.

We gratefully acknowledge the aid of Grace Rowe, of the M. I. T. Laboratory for Nuclear Science and Engineering, who did the drafting work required in the revision of the original compilation and in the preparation of these curves for publication. This work was supported in part by the U. S. Navy Department, under contract N5-ori-78.

Note added in proof.—Since the completion of this compilation, many papers have appeared concerning various aspects of neutron cross-section theory and measurement. Thus, the theory of neutron resonances has been further investigated,[61] a method of using the pile for the meas-

[61] E. P. Wigner and L. Eisenbud, Phys. Rev. **72**, 29 (1947).

urement of thermal neutron absorption cross sections has been described,[62] the use of crystal spectrometers for velocity selection has been improved,[63–65] and the use of the long counter for the detection of intermediate energy neutrons has been reported.[66] Interference effects have been utilized to investigate further such phenomena as the phase change in neutron scattering[67] and the nuclear spin dependence of the neutron scattering cross section.[68] Slow neutron interference effects have also been applied to the investigation of the strength of the interaction between neutrons and electrons.[69] The properties of the high energy neutrons ($E \sim 100$ Mev) produced by ultra high energy accelerators are now being studied.[70]

Among the cross-section data which were unpublished when these curves were assembled, many have now appeared in the literature. Thus, references are now available for the undocumented data in Figs. 2,[71] 5,[72] 9,[21] 21,[47] 44,[64] 46,[63, 65] 51,[73] 55,[64] 56,[20, 64] 59,[65] 61,[20, 22, 64] and 68.[74] New data have been reported for the high energy cross section of carbon (Fig. 11)[71] and the low energy cross section of iridium (Fig. 59).[64]

R. F. Taschek has kindly called to our attention that the data on σ_p of sulfur (Figs. 24, 26), attributed by us to him, are due to A. O. Hanson and E. D. Klema. Also, the value of Γ for the 0.176-ev resonance in cadmium is erroneously quoted in Fig. 46; it should have been 0.115 ev.

[62] H. L. Anderson, E. Fermi, A. Wattenberg, G. L. Weil, and W. H. Zinn, Phys. Rev. **72**, 16 (1947).
[63] W. H. Zinn, Phys. Rev. **71**, 752 (1947).
[64] W. J. Sturm, Phys. Rev. **71**, 757 (1947).
[65] R. B. Sawyer, E. O. Wollan, S. Bernstein, and K. C. Peterson, Phys. Rev. **72**, 109 (1947).
[66] A. O. Hanson and J. L. McKibben, Phys. Rev. **72**, 673 (1947).
[67] E. Fermi and L. Marshall, Phys. Rev. **71**, 915 (1947).
[68] E. Fermi and L. Marshall, Phys. Rev. **72**, 408 (1947).
[69] W. W. Havens, Jr., I. I. Rabi, and L. J. Rainwater, Phys. Rev. **72**, 634 (1947).
[70] W. M. Powell, Phys. Rev. **72**, 739(A) (1947).
[71] W. Sleator, Jr., Phys. Rev. **72**, 207 (1947).
[72] T. A. Hall and P. G. Koontz, Phys. Rev. **72**, 196 (1947).
[73] W. B. Jones, Jr., Phys. Rev. **72**, 362 (1947).
[74] E. D. Klema, Phys. Rev. **72**, 88 (1947).